Chapter 10

Neutrino scattering Cross Sections from Hadrons: Quasielastic Scattering

10.1 Introduction

In the last chapter, we have discussed how to calculate the cross sections for the scattering of two point-like particles. Now the question arises, what happens when an electron interacts with a charge which is distributed in space like the one shown in Figure 10.1. The standard technique to measure the charge distribution and get information about the structure of the hadron is to measure the differential/total scattering cross sections of electron with a hadron and compare it with the cross section of electron scattering with a spinless ($J = 0$) point target (known as Mott scattering cross section). The ratio of these two is generally expressed as

$$\frac{\left(\frac{d\sigma}{d\Omega}\right)_{\text{extended}}}{\left(\frac{d\sigma}{d\Omega}\right)_{\text{Mott}}} = \left|F(q^2)\right|^2, \tag{10.1}$$

where $F(q^2)$, in literature, is known as the form factor. This accounts for the spatial extent of the scatterer. $F(q^2)$ not only tells about the distribution of the charge in space but using it, one can estimate the size of the target particle as well as its charge distribution and density of magnetization. Thus, for an extended charge distribution, the probability amplitude for a point-like scatterer is modified by a form factor.

https://doi.org/10.1017/9781108489065.011 Published online by Cambridge University Press

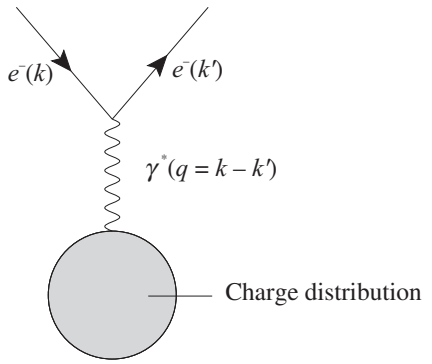

Figure 10.1 Interaction of an electron with a charge distribution.

10.2 Physical Significance of the Form Factor

Consider the elastic scattering of a "spinless" electron from a static "spinless" point object having charge $Z|e|$. In the Born approximation, where the perturbation is assumed to be weak, the scattering amplitude is written as

$$f_B = \int \psi^*_{\vec{k}'}(\vec{r})V(\vec{r})\psi_{\vec{k}}(\vec{r})d\vec{r}, \quad V(\vec{r}) = -\frac{Ze^2}{4\pi r} \tag{10.2}$$

where $\psi_{\vec{k}}$ and $\psi_{\vec{k}'}$ are the wave functions of the initial and final electron with momentum $\vec{k}$ and $\vec{k}'$, respectively. These waves are assumed to be plane waves such that

$$f_B = \int e^{i\vec{q}\cdot\vec{r}}V(\vec{r})d\vec{r}, \qquad \text{where} \quad \vec{q} = \vec{k} - \vec{k}'. \tag{10.3}$$

Instead of a point charge distribution, if we assume an extended charge distribution $Z|e|\rho(\vec{r})$ with normalization $\int \rho(\vec{r})d\vec{r} = 1$, then the potential felt by the electron located at $\vec{r}$ is given by

$$V(\vec{r}) = -\frac{Z|e^2|}{4\pi}\int \frac{\rho(\vec{r}')}{|\vec{r} - \vec{r}'|}d\vec{r}', \tag{10.4}$$

where $\vec{r}'$ is the maximum range of the charge distribution. The scattering amplitude modifies to

$$f_B = -\frac{Z|e^2|}{4\pi}\int e^{i\vec{q}\cdot\vec{r}}\int \frac{\rho(\vec{r}')}{|\vec{r} - \vec{r}'|}d\vec{r}\, d\vec{r}'. \tag{10.5}$$

Assuming $\vec{R} = \vec{r} - \vec{r}'$, which leads to $d\vec{R} = d\vec{r}$,

$$f_B = -\frac{Z|e^2|}{4\pi}\int \frac{e^{i\vec{q}\cdot\vec{R}}}{|\vec{R}|}d\vec{R}\Big[\int e^{i\vec{q}\cdot\vec{r}'}\rho(\vec{r}')d\vec{r}'\Big]. \tag{10.6}$$

The term in the square brackets on the right-hand side of Eq. (10.6) is known as the form factor, which is nothing but the Fourier transform of the charge density distribution, given as

$$F(\vec{q}) = \int e^{i\vec{q}\cdot\vec{r}'}\rho(\vec{r}')d\vec{r}'. \tag{10.7}$$

https://doi.org/10.1017/9781108489065.011 Published online by Cambridge University Press

In field theory, if we consider the scattering of a spin $\frac{1}{2}$ electron from an external electromagnetic field (shown in Figure 10.2), the electromagnetic field in the momentum space is written as

$$A^{\mu}_{\rm em}(\vec{q}) = \frac{1}{(2\pi)^3}\int e^{i\vec{q}\cdot\vec{r}} A^{\mu}_{\rm em}(\vec{r})d\vec{r}, \tag{10.8}$$

where $\vec{q} = \vec{k}' - \vec{k}$ is the momentum transferred from the field source (represented by a cross in Figure 10.2) to the electron and $A^{\mu}_{\rm em}(\vec{q})$ is the electromagnetic field in the momentum space. The transition amplitude, following the Feynman rules, may be written as

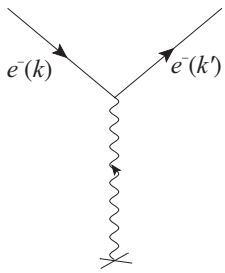

Figure 10.2 Feynman diagram in momentum space for electron scattering from an external source of electromagnetic field.

$$\mathcal{M} = e\bar{u}(\vec{k}')\gamma_{\mu}u(\vec{k})A^{\mu}_{\rm em}(\vec{q}), \tag{10.9}$$

where $u(\vec{k})$ and $\bar{u}(\vec{k}')$ are, respectively, the Dirac spinors for the incoming electron and the adjoint Dirac spinor for the outgoing electron. Square of this amplitude is given as

$$|\mathcal{M}|^2 = e^2|\bar{u}(\vec{k}')\not{A}_{\rm em}u(\vec{k})|^2. \tag{10.10}$$

Using Coulomb gauge for the electromagnetic field created by a point charge, that is,

$$A^{\mu}_{\rm em}(\vec{x}) = \left(\frac{Ze}{4\pi|\vec{x}|}, 0, 0, 0\right), \ \ (\text{innaturalunits}) \tag{10.11}$$

written in the momentum space by using Fourier transform as

$$A^{\mu}_{\rm em}(\vec{q}) = \left(\frac{Ze}{|\vec{q}|^2}, 0, 0, 0\right), \tag{10.12}$$

we obtain the expression for the differential scattering cross section for a static external source in the massless limit of the electron, using the general expression of $\frac{d\sigma}{d\Omega}$ (given in Appendix E) as

$$\left.\frac{d\sigma}{d\Omega}\right|_{\rm Mott} = \frac{\alpha^2}{4E^2\sin^4\frac{\theta}{2}}\cos^2\frac{\theta}{2}. \tag{10.13}$$

Instead of a point charge distribution, if we assume the nucleus to have a spherical charge distribution $Ze\rho(r)$ with $\int \rho(r)d\vec{r} = 1$, then the expression for the differential cross section is obtained as

$$\frac{d\sigma}{d\Omega} = \left(\frac{d\sigma}{d\Omega}\right)_{\rm Mott}|F(\vec{q})|^2, \tag{10.14}$$

https://doi.org/10.1017/9781108489065.011 Published online by Cambridge University Press

where $F(q^2)$ is the Fourier transform of the charge density distribution and we may write

$$\begin{aligned} F(q^2) &= \int_{r=0}^{\infty}\int_{\cos\theta=-1}^{+1}\int_{\phi=0}^{2\pi} r^2 dr\, d\cos\theta\, d\phi\, \rho(r)\, e^{i|\vec{q}||\vec{r}|\cos\theta} \\ &= \frac{4\pi}{q^2}\int_{r=0}^{\infty}(qr)\sin(qr)\rho(r)dr;\ \ |\vec{q}| = q \\ &= \frac{4\pi}{q^2}\int_{r=0}^{\infty}\left(q^2r^2 - \frac{q^4r^4}{6} + ...\right)\rho(r)dr. \end{aligned} \tag{10.15}$$

In the limit of small angle scattering, using Eq. (10.15), $\frac{dF}{dq^2}$ may be written as

$$\begin{aligned} \left.\frac{dF(q^2)}{dq^2}\right|_{q^2=0} &= -\frac{1}{6}\int_{r=0}^{\infty} r^2(4\pi r^2\rho(r))dr = -\frac{1}{6}\langle r^2\rangle \\ \Rightarrow \qquad \langle r^2\rangle &= -6\left.\frac{dF(q^2)}{dq^2}\right|_{q^2=0}, \end{aligned} \tag{10.16}$$

where $\langle r^2\rangle$ is the mean charge radius squared of the scatterer, resulting in $r_{\rm rms} = \sqrt{\langle r^2\rangle}$, which gives the rms charge radius of the scatterer.

If the charge distribution has an exponential form like $\rho(r) = \rho(0)e^{-m_v r}$, then the form factor $F(q^2)$ turns out to be:

$$\begin{aligned} F(q^2) &= \frac{4\pi}{q^2}\int_{r=0}^{\infty}(qr)\sin(qr)\rho(0)e^{-m_v r}dr \\ &= \frac{4\pi}{q^2}\int_{r=0}^{\infty}(qr)\frac{e^{-(m_v-iq)r} - e^{-(m_v+iq)r}}{2i}\rho(0)dr \\ &= \frac{8\pi\rho_0}{m_v^3}\frac{1}{\left(1+\frac{q^2}{m_v^2}\right)^2} \end{aligned}$$

known as the dipole form factor with m_v as the vector dipole mass.

For a Yukawa type charge distribution $\rho(r) = \rho(0)\frac{e^{-mr}}{r}$, the form factor $F(q^2)$ is of a monopole form:

$$F(q^2) \propto \frac{1}{\left(1-\frac{q^2}{m^2}\right)},$$

where m^2 is in the units of q^2.

In the next section, we will see how, in the theoretical formalism, the scattering cross sections are expressed in terms of the form factors. For simplicity, this has been demonstrated by taking a pion (spin 0) target, which is described by a single form factor $F_\pi(q^2)$. Experimentally, however, one measures the differential or the total scattering cross sections and from there, information about the form factors is obtained. The best description of the

https://doi.org/10.1017/9781108489065.011 Published online by Cambridge University Press

experimental data by a given set of form factor(s) using least square fitting method determines the parameterization of the form factor. With these form factors, other information like the charge density distribution, size of the scatterer, etc. are obtained.

10.3 $e^- - \pi^\pm$ Elastic Scattering

Elastic electron–pion scattering takes place via the exchange of a virtual photon in the reaction

$$e^-(k) + \pi^\pm(p) \longrightarrow e^-(k') + \pi^\pm(p'),$$

where k, k' and p, p' are the incoming and outgoing momenta of the electrons and pions, respectively.

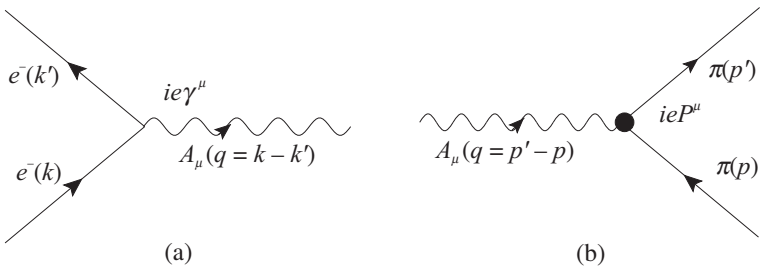

Figure 10.3 (a) Leptonic and (b) hadronic vertices for the $e^- - \pi^\pm$ elastic scattering.

When an electron interacts with a photon field (Figure 10.3(a)), the interaction Lagrangian is given by

$$\mathcal{L}_I^e = -\bar{\psi}(\vec{k}')e\gamma^\mu\psi(\vec{k})A_\mu, \tag{10.17}$$

and when a pion interacts with a photon field (Figure 10.3(b)), the interaction Lagrangian is given by

$$\mathcal{L}_I^\pi = -j_\mu^\pi A^\mu \qquad \text{with} \tag{10.18}$$

$$j_\mu^\pi = f_1(p^2, p'^2, p\cdot p')P_\mu + f_2(p^2, p'^2, p\cdot p')q_\mu, \tag{10.19}$$

where $P^\mu = p^\mu + p'^\mu$ and $f_1(p^2, p'^2, p\cdot p')$ and $f_2(p^2, p'^2, p\cdot p')$ are unknown functions which depend upon the scalar quantities constructed from the four momenta of the incoming and the outgoing pions p_μ and p'_μ, respectively, that is, p^2, p'^2 and $p\cdot p'$. Since $p^2 = p'^2 = m_\pi^2$ and $p\cdot p' = m_\pi^2 - \frac{q^2}{2}$, only q^2 is a variable quantity. Therefore, in the case of elastic scattering, the form factors are the function of q^2 only.

Conservation of the vector current at the hadronic vertex, that is, $\partial^\mu j_\mu^\pi = 0$ leads to $f_2(q^2) = 0$, and one is left only with one scalar function $f_1(q^2)$. For simplicity, we rename this form factor $f_1(q^2)$ as $F_\pi(q^2)$. Using the Lagrangians defined in Eqs. (10.17) and (10.18),

https://doi.org/10.1017/9781108489065.011 Published online by Cambridge University Press

the transition amplitude for the process $e^-\pi^+ \to e^-\pi^+$, as depicted in Figure 10.4, is written as

$$\begin{aligned} -i\mathcal{M} &= \underbrace{\bar{u}(\vec{k}')ie\gamma^\mu u(\vec{k})}_{\text{leptonic current}} \underbrace{\left(\frac{-ig_{\mu\nu}}{q^2}\right)}_{\text{propagator}} \underbrace{ieP_\mu F_\pi(q^2)}_{\text{hadronic current}} \\ \Rightarrow \qquad \mathcal{M} &= -\frac{e^2}{q^2}\left[\bar{u}(\vec{k}')\gamma^\mu u(\vec{k})\right] P_\mu F_\pi(q^2). \end{aligned} \tag{10.20}$$

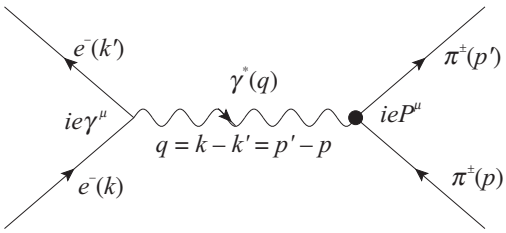

Figure 10.4 Feynman diagram for $e^- - \pi^\pm$ scattering. The quantities in the bracket represent the four momenta of the particles.

The transition matrix element squared is obtained following the same formalism as mentioned in Chapter 9, as

$$\overline{\sum}\sum |\ \mathcal{M}\ |^2 = \frac{e^4}{q^4}\frac{1}{2}\overline{\sum}\sum |\ \left[\bar{u}(\vec{k}')\gamma^\mu u(\vec{k})\right]\ |^2\ P_\mu P_\nu F_\pi^2(q^2) \tag{10.21}$$

where $P = p + p' = 2p + q$. In the massless limit of the electron, Eq. (10.21) reduces to

$$\overline{\sum}\sum |\ \mathcal{M}\ |^2 = \frac{4e^4}{q^4}(4(k\cdot p)(k'\cdot p) + q^2 m_\pi^2)F_\pi^2(q^2), \tag{10.22}$$

where pion is on the mass shell, that is, $p^2 = m_\pi^2$. Using the expression of the differential scattering cross section in the Lab frame (Appendix E), where $p = (m_\pi, \vec{0}), k\cdot p = m_\pi E$, $k'\cdot p = m_\pi E'$, $\frac{d\sigma}{d\Omega}\ |_{\text{Lab}}$ is obtained as

$$\left.\frac{d\sigma}{d\Omega}\right|_{\text{Lab}} = \frac{1}{64\pi^2 m_\pi E}\overline{\sum}\sum|\mathcal{M}|^2\frac{|\vec{k}'|^3}{((E+m_\pi)|\vec{k}'|^2 - \vec{k}\cdot\vec{k}'E')} \tag{10.23}$$

which may be further solved to give

$$\left.\frac{d\sigma}{d\Omega}\right|_{\text{Lab}} = \frac{\alpha^2}{4\ E^2\sin^4\frac{\theta}{2}}\frac{E'}{E}F_\pi^2(q^2)\cos^2\frac{\theta}{2}. \tag{10.24}$$

In the experimental measurements of $e^- - \pi^\pm$ scattering as well as through some other inelastic processes like $e^- p \to e^-\pi^+ n$, it has been observed that with a form of

$$F_\pi(q^2) = \frac{1}{1 - \langle r_\pi^2\rangle\frac{q^2}{6}},$$

https://doi.org/10.1017/9781108489065.011 Published online by Cambridge University Press

the experimental data may be explained using $r_\pi^{\rm rms} = \sqrt{\langle r_\pi^2 \rangle} = 0.657 \pm 0.012$ fm.

Thus, for the elastic $e^-\pi^+$ scattering, the cross section is described in terms of a form factor. When we compare this cross section (given in Eq. (10.24)) with the Mott scattering cross section given in Eq. (10.13), in the case of $e^-\pi^+$ scattering, the modifications are the presence of $F_\pi^2(q^2)$, due to the structure of the pion and $\frac{E'}{E}$, due to the recoil of the pion. Moreover, when the cross section given in Eq. (10.24) is compared with the cross section obtained for the $e^-\mu^-$ scattering (discussed in Chapter 9), we realize that an additional contribution, in the case of $e^-\mu^-$ scattering, arises due to the spin of the muon. In the next section, we will see how the form factors play an important role in e^-p scattering where the proton is a spin $\frac{1}{2}$ particle similar to that of a muon but the proton will also have a structure.

10.4 Electromagnetic Scattering of Electrons with Nucleons

10.4.1 Matrix element and form factors

First, let us consider the electromagnetic scattering of electrons with protons expressed as

$$e^-(k) + p(p) \longrightarrow e^-(k') + p(p'),$$

where k, k' and p, p' are the incoming and outgoing momenta of the electron and proton, respectively. The Lagrangian at the leptonic and hadronic vertices for the electron and the proton (presented in Figure 10.5) interacting with a photon field is given as

$$\begin{aligned} \mathcal{L}_I^l &= -e\overline{\psi}(\vec{k}')\gamma^\mu A_\mu \psi(\vec{k}), \\ \mathcal{L}_I^h &= -e\overline{\psi}(\vec{p}')\Gamma^\mu A_\mu \psi(\vec{p}), \end{aligned}$$

where γ^μ is a Dirac four vector and Γ^μ shows our lack of knowledge about the hadronic vertex represented by a blob in Figure 10.5(b). The transition amplitude $\mathcal{M}$ has to be a Lorentz scalar. Since the leptonic vertex is a four vector, the hadronic vertex also has to be a four vector (Γ_μ). To construct Γ_μ at the hadronic vertex, the two independent four vectors are p_μ and p'_μ. Since the proton is a spin $\frac{1}{2}$ Dirac particle and the interaction is electromagnetic in nature where parity is conserved, the most general form of the hadronic current with possible bilinear

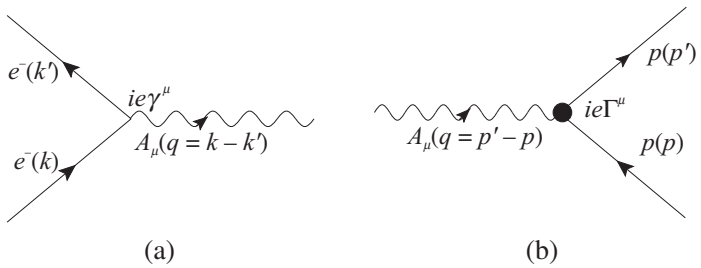

Figure 10.5 (a) Leptonic and (b) hadronic vertices for the elastic e^-p scattering.

https://doi.org/10.1017/9781108489065.011 Published online by Cambridge University Press

covariants (see Appendix A) transforming as a vector can be constructed from p_μ, p'_μ, γ_μ and $\sigma_{\mu\nu}(=\frac{i}{2}[\gamma_\mu,\gamma_\nu])$ operators and written as

$$\begin{aligned}\Gamma^\mu &= A(p^2,p'^2,p\cdot p')\gamma^\mu + B(p^2,p'^2,p\cdot p')p'^\mu + C(p^2,p'^2,p\cdot p')p^\mu \\ &+ iD(p^2,p'^2,p\cdot p')\sigma^{\mu\nu}p'_\nu + iE(p^2,p'^2,p\cdot p')\sigma^{\mu\nu}p_\nu. \end{aligned} \tag{10.25}$$

Here, A, B, C, D, and E are undetermined scalar functions depending upon q^2 in the case of the elastic scattering.

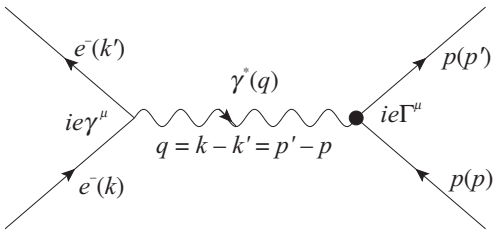

Figure 10.6 Feynman diagram for e^-p scattering. The quantities in the bracket represent the four momenta of the particles.

Invariant amplitude for the elastic e^-p scattering, depicted in Figure 10.6, is written as

$$-i\mathcal{M} = \underbrace{(i\,j^{e(\mu)})}_{\text{leptonic current}} \underbrace{\left(-i\frac{g_{\mu\nu}}{q^2}\right)}_{\text{propagator}} \underbrace{(i\,J^{p(\mu)})}_{\text{hadronic current}},$$

where

$$j^{e(\mu)} = \bar{u}(\vec{k}')\, e\, \gamma^\mu u(\vec{k}), \tag{10.26}$$

$$J^{p(\mu)} = \bar{u}(\vec{p}')\, e\, \Gamma^\mu u(\vec{p}). \tag{10.27}$$

Using the currents defined in Eqs. (10.26) and (10.27), the transition amplitude is obtained as

$$\mathcal{M} = -\frac{e^2}{q^2}\left[\bar{u}(\vec{k}')\gamma^\mu u(\vec{k})\right]\left[\bar{u}(\vec{p}')\Gamma_\mu u(\vec{p})\right], \tag{10.28}$$

with Γ^μ as given in Eq. (10.25).

Since Γ^μ is constructed from the four vectors available at the hadronic vertex using the bilinear covariants and there is no definite form of Γ^μ, we may rewrite Eq. (10.25) as

$$\begin{aligned}\Gamma^\mu &= A(q^2)\gamma^\mu + B'(q^2)(p'-p)^\mu + C'(q^2)(p'+p)^\mu \\ &+ iD'(q^2)\sigma^{\mu\nu}(p'-p)_\nu + iE'(q^2)\sigma^{\mu\nu}(p'+p)_\nu. \end{aligned} \tag{10.29}$$

The last term of Eq. (10.29) may be expressed as

$$\begin{aligned}\bar{u}(\vec{p}')[i\sigma^{\mu\nu}(p'+p)_\nu]u(\vec{p}) &= \bar{u}(\vec{p}')[-\frac{1}{2}(\gamma^\mu\gamma^\nu - \gamma^\nu\gamma^\mu)(p'+p)_\nu]u(\vec{p}) \\ &= -\bar{u}(\vec{p}')[(p'-p)^\mu]u(\vec{p}), \end{aligned} \tag{10.30}$$

https://doi.org/10.1017/9781108489065.011 Published online by Cambridge University Press

where we have used Dirac equations, that is, $(\not{p} - M)u(\vec{p}) = 0$ and $\bar{u}(\vec{p}')(\not{p}' - M) = 0$. From Eq. (10.30), it may be noticed that the last term in Eq. (10.29) can be written in terms of the second term in Eq. (10.29). Similarly, we obtain

$$\bar{u}(\vec{p}')[i\sigma^{\mu\nu}(p'-p)_\nu]u(\vec{p}) \quad = \quad \bar{u}(\vec{p}')[2M\gamma^\mu - (p'+p)^\mu]u(\vec{p}), \tag{10.31}$$

which is called Gordon decomposition.

Therefore, Eq. (10.31) can be rewritten as

$$\bar{u}(\vec{p}')(p'+p)^\mu u(\vec{p}) \quad = \quad \bar{u}(\vec{p}')[2M\gamma^\mu - i\sigma^{\mu\nu}(p'-p)_\nu]u(\vec{p}). \tag{10.32}$$

Thus, it may be deduced that out of the five terms from which Γ^μ is constructed, only three are linearly independent. Using Eqs. (10.30) and (10.32) in Eq. (10.29), we obtain

$$\Gamma^\mu = \gamma^\mu(A(q^2) + 2MC'(q^2)) + i\sigma^{\mu\nu}q_\nu(D'(q^2) - C'(q^2)) + q^\mu(B'(q^2) - E'(q^2)). \tag{10.33}$$

Redefining the form factors, one can obtain Γ^μ as

$$\Gamma^\mu \quad = \quad \gamma^\mu F_1(q^2) + i\sigma^{\mu\nu}q_\nu\frac{F_2(q^2)}{2M} + q^\mu\frac{F_3(q^2)}{M}. \tag{10.34}$$

Applying current conservation in momentum space, that is, $q_\mu J^{p(\mu)} = 0$, where $J^{p(\mu)}$ is defined in Eq. (10.27) with Γ^μ given in Eq. (10.34):

$$q_\mu J^{p(\mu)} = q_\mu\bar{u}(\vec{p}')e\left[\gamma^\mu F_1(q^2) + i\sigma^{\mu\nu}q_\nu\frac{F_2(q^2)}{2M} + q^\mu\frac{F_3(q^2)}{M}\right]u(\vec{p}) = 0$$

$$\Rightarrow \bar{u}(\vec{p}')e\left[F_1(q^2)(\not{p}' - \not{p}) - \frac{1}{2}(\gamma^\mu\gamma^\nu - \gamma^\nu\gamma^\mu)q_\mu q_\nu\frac{F_2(q^2)}{2M} + q^2\frac{F_3(q^2)}{M}\right]u(\vec{p}) = 0. \tag{10.35}$$

Therefore, from current conservation, the first term on the left-hand side is zero when Dirac equation is applied; the second term will give $q^2 - q^2 = 0$; and from the last term, $F_3(q^2) = 0$ as $q^2 \neq 0$. Hence, the hadronic current becomes

$$\bar{u}(\vec{p}')e\Gamma_\mu u(\vec{p}) \quad = \quad \bar{u}(\vec{p}')e\left[\gamma_\mu F_1(q^2) + \frac{i\sigma_{\mu\nu}q^\nu}{2M}F_2(q^2)\right]u(\vec{p}). \tag{10.36}$$

Using Gordon decomposition in Eq. (10.36),

$$\bar{u}(\vec{p}')e\Gamma_\mu u(\vec{p}) \quad = \quad \bar{u}(\vec{p}')e\left[\gamma_\mu\left\{F_1(q^2) + F_2(q^2)\right\} - \frac{1}{2M}P_\mu F_2(q^2)\right]u(\vec{p}), \tag{10.37}$$

where we have used Eq. (10.31).

$F_1(q^2)$ and $F_2(q^2)$ are, respectively, known as the Dirac and Pauli form factors. In this section, we will discuss the scattering of electrons with free protons; therefore, in the rest of the text, we call these form factors as $F_1^p(q^2)$ and $F_2^p(q^2)$. Moreover, if the scattering of electrons takes place with free neutrons, then the only change in Eq. (10.37) is in the form factors; for the $e^- n$ scattering, $F_1^n(q^2)$ and $F_2^n(q^2)$ are the Dirac and Pauli neutron form factors.

Besides, hermiticity of electromagnetic current demands that

$$\langle p|j_\mu^\dagger|p'\rangle \quad = \quad \langle p'|j_\mu|p\rangle^* = \langle p|j_\mu|p'\rangle. \tag{10.38}$$

https://doi.org/10.1017/9781108489065.011 Published online by Cambridge University Press

From Eq. (10.37), we have

$$\Rightarrow \{\bar{u}(\vec{p}\,')e\Gamma^{\mu}u(\vec{p})\}^{*} = e\left[u^{\dagger}(\vec{p}\,')\left\{\gamma^{0}\gamma^{\mu}\left\{F_1(q^2)+F_2(q^2)\right\}-\gamma^{0}\frac{1}{2M}P^{\mu}F_2(q^2)\right\}u(\vec{p})\right]^{*}$$
$$= u^{\dagger}(\vec{p})e\left[\gamma^{\mu\dagger}\gamma^{0\dagger}\left\{F_1^{*}(q^2)+F_2^{*}(q^2)\right\}-\gamma^{0\dagger}\frac{1}{2M}P^{\mu}F_2^{*}(q^2)\right]u(\vec{p}\,')$$
$$= \bar{u}(\vec{p})e\left[\gamma^{\mu}\left\{F_1^{*}(q^2)+F_2^{*}(q^2)\right\}-\frac{1}{2M}P^{\mu}F_2^{*}(q^2)\right]u(\vec{p}\,'), \quad (10.39)$$

where we have used $(\gamma^0\gamma^\mu)^\dagger = \gamma^0\gamma^\mu$. Requirement of Eq. (10.38) demands that when Eq. (10.37) and Eq. (10.39) are compared, we must have $F_1(q^2) = F_1^*(q^2)$; $F_2(q^2) = F_2^*(q^2)$. This implies that the form factors $F_1(q^2)$ and $F_2(q^2)$ are real.

10.4.2 Physical interpretation of the form factors

In order to give a physical interpretation of the electromagnetic form factors $F_1(q^2)$ and $F_2(q^2)$, it is demonstrative to evaluate the matrix elements of the electromagnetic currents in the Breit frame.

The Breit frame (or the brickwall frame), depicted in Figure 10.7 is defined as the frame in which the target of mass M is assumed to be very massive in comparison to the mass of the projectile m such that there is no transfer of energy to the target, that is, $E_p = E_{p'}$ and the only change is in the direction of the projectile, that is, $\vec{p} + \vec{p}\,' = 0 \Rightarrow \vec{p}\,' = -\vec{p}$. In this frame, the four momentum transfer q becomes $(q_0 = 0, \vec{q} = -2\vec{p})$.

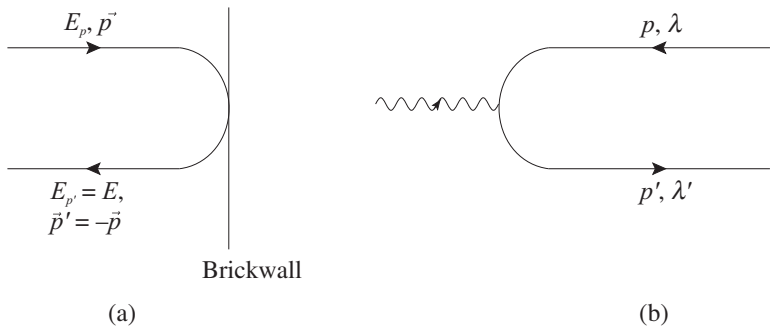

Figure 10.7 The brickwall frame.

We recall that the expression for the hadronic current J^μ is given by

$$J^{\mu} = \bar{u}(\vec{p}\,')e\left[\gamma^{\mu}(F_1(q^2)+F_2(q^2)) - \frac{P^{\mu}}{2M}F_2(q^2)\right]u(\vec{p}).$$

In the Breit frame, the zeroth component of the current four vector J^μ becomes

$$J^{0} = \bar{u}(\vec{p}\,')e\left[\gamma^{0}(F_1(q^2)+F_2(q^2)) - \frac{P^{0}}{2M}F_2(q^2)\right]u(\vec{p}), \quad (10.40)$$

https://doi.org/10.1017/9781108489065.011 Published online by Cambridge University Press

where $P^0 = E_p + E_{p'} = 2E_p$, resulting in

$$\bar{u}(-\vec{p})\gamma^0 u(\vec{p}) = u^\dagger(-\vec{p})u(\vec{p}) = 2M, \tag{10.41}$$

$$\bar{u}(-\vec{p})u(\vec{p}) = u^\dagger(-\vec{p})\gamma^0 u(\vec{p}) = 2E_p. \tag{10.42}$$

Using Eqs. (10.41) and (10.42) in Eq. (10.40), the zeroth component of the hadronic current becomes

$$J^0 = \rho = 2Me\left(F_1(q^2) + \frac{q^2}{4M^2}F_2(q^2)\right).$$

The quantity in the bracket is identified as the Sachs electric form factor $G_E(q^2)$ as

$$\rho = 2Me\, G_E(q^2). \tag{10.43}$$

The ith component of the hadronic current becomes

$$\vec{J} = \bar{u}(-\vec{p})e\left[\gamma^i(F_1(q^2) + F_2(q^2)) - \frac{\vec{P}}{2M}F_2(q^2)\right]u(\vec{p}). \tag{10.44}$$

Since $\vec{P} = \vec{p}\,' + \vec{p} = 0$, Eq. (10.44) becomes

$$\begin{aligned}\vec{J} &= \bar{u}(-\vec{p})e\left[\gamma^i(F_1(q^2) + F_2(q^2))\right]u(\vec{p}) \\ &= -e\,\chi^{s'\dagger}(\vec{\sigma}\times\vec{q})\chi^s G_M(q^2).\end{aligned} \tag{10.45}$$

$F_1(q^2) + F_2(q^2)$ is known as the Sachs magnetic form factor $G_M(q^2)$.

Therefore, from Eqs. (10.43) and (10.45), it may be deduced that in the Breit frame, $J^0(= \rho)$ and $\vec{J}$ are related to the electric and magnetic Sachs form factors $G_E(q^2)$ and $G_M(q^2)$, respectively. This means that in the Breit frame, $G_E(q^2)$ and $G_M(q^2)$ are, respectively, the Fourier transforms of the charge density and the density of magnetization.

These Sachs form factors of the nucleon are expressed as

$$G_E^N(q^2) = F_1^N(q^2) + \frac{q^2}{4M^2}F_2^N(q^2), \tag{10.46}$$

$$G_M^N(q^2) = F_1^N(q^2) + F_2^N(q^2). \tag{10.47}$$

Equivalently, $F_1^N(q^2)$, $F_2^N(q^2)$ and their combination $F_M^N(q^2)(= F_1^N(q^2) + F_2^N(q^2))$ may be redefined in terms of $G_E^N(q^2)$ and $G_M^N(q^2)$ as

$$F_1^N(q^2) = \frac{G_E^N(q^2) + \tau G_M^N(q^2)}{1+\tau}, \tag{10.48}$$

$$F_2^N(q^2) = \frac{G_M^N(q^2) - G_E^N(q^2)}{1+\tau}, \tag{10.49}$$

$$F_M^N(q^2) = F_1^N(q^2) + F_2^N(q^2) = G_M^N(q^2), \qquad \text{where } \tau = -\frac{q^2}{4M^2}. \tag{10.50}$$

https://doi.org/10.1017/9781108489065.011 Published online by Cambridge University Press

10.4.3 Cross sections and the Rosenbluth separation

With Γ_μ defined in Eq. (10.36), the transition matrix element squared may be obtained as

$$\overline{\sum}\sum \mid \mathcal{M} \mid^2 = \frac{e^4}{q^4}\overline{\sum}\sum \mid \left[\bar{u}(\vec{k}')\gamma^\mu u(\vec{k})\right] \mid^2 \mid \left[\bar{u}(\vec{p}')\Gamma_\mu u(\vec{p})\right] \mid^2,$$

where the sum over the spin of the final state particles and the average over the spin of the initial state particles have been taken into account, resulting in

$$\begin{aligned}\overline{\sum}\sum \mid \mathcal{M} \mid^2 = & \frac{e^4}{q^4}\cdot\frac{1}{2}\cdot\frac{1}{2}\cdot Tr\left[(\not{k}'+m_e)\gamma^\mu(\not{k}+m_e)\gamma^\nu\right] \\ & Tr\left((\not{p}'+M)\left[\gamma_\mu\left\{F_1^p(q^2)+F_2^p(q^2)\right\}-\frac{1}{2M}P_\mu F_2^p(q^2)\right]\right. \\ & \left.(\not{p}+M)\left[\gamma_\nu\left\{F_1^p(q^2)+F_2^p(q^2)\right\}-\frac{1}{2M}P_\nu F_2^p(q^2)\right]\right).\end{aligned}$$

Using $\left\{F_1^p(q^2)+F_2^p(q^2)\right\} = F_M^p(q^2)$, $\overline{\sum}\sum \mid \mathcal{M} \mid^2$ may be rewritten as

$$\begin{aligned}\overline{\sum}\sum \mid \mathcal{M} \mid^2 = & \frac{4e^4}{q^4}\cdot\left[k^\mu k'^\nu + k'^\mu k^\nu - (k\cdot k' - m_e^2)g^{\mu\nu}\right] \\ & \times \left(F_M^{p\,2}(q^2)\left[p_\mu p'_\nu + p'_\mu p_\nu - (p\cdot p' - M^2)g_{\mu\nu}\right]\right. \\ & - \frac{F_M^p(q^2)F_2^p(q^2)}{2M}M\left(p'_\mu P_\nu + P_\mu p'_\nu + p_\mu P_\nu + P_\mu p_\nu\right) \\ & \left. + \frac{F_2^{p2}(q^2)}{4M^2}\left(p\cdot p' + M^2\right)P_\mu P_\nu\right). \end{aligned} \tag{10.51}$$

The expression for $\overline{\sum}\sum \mid \mathcal{M} \mid^2$ becomes

$$\begin{aligned}\overline{\sum}\sum \mid \mathcal{M} \mid^2 = \frac{8e^4}{q^4}\Bigg\{ & F_M^{p\,2}(q^2)\left[k\cdot pk'\cdot p' + k\cdot p'k'\cdot p - M^2 k\cdot k' - m_e^2 p\cdot p' + 2m_e^2 M^2\right] \\ & - F_M^p(q^2)\frac{F_2^p(q^2)}{2M}M\left[2P\cdot kP\cdot k' - (k\cdot k' - m_e^2)P^2\right] \\ & + \frac{F_2^{p2}(q^2)}{4M^2}\frac{1}{2}P^2\left[P\cdot kP\cdot k' - \frac{(k\cdot k' - m_e^2)}{2}P^2\right]\Bigg\}.\end{aligned}$$

https://doi.org/10.1017/9781108489065.011 Published online by Cambridge University Press

Defining the four momentum transfer, $q = k - k' = p' - p$, and the sum of the momenta, $P = p + p'$ and applying the momentum conservation $k + p = k' + p'$, which gives $p' = k + p - k'$, the transition matrix element squared may be obtained as

$$\begin{aligned}\overline{\sum}\sum \mid \mathcal{M} \mid^2 \;=\; & \frac{8e^4}{q^4}\Bigg\{ {F_M^p}^2(q^2)\left[-2k\cdot p\left(m_e^2 - k'\cdot p\right) + 2m_e^2 k'\cdot p + m_e^2 M^2\right. \\ & -\; \left. k\cdot k'\left(-k\cdot p + k'\cdot p + M^2\right)\right] - MF_M^p(q^2)\frac{F_2^p(q^2)}{2M}\left[4\left(m_e^2 M^2 - M^2 k\cdot k'\right.\right. \\ & +\; \left.\left. 2k\cdot pk'\cdot p\right)\right] + \frac{{F_2^p}^2(q^2)}{4M^2}\left[2\left(k\cdot p - k'\cdot p + 2M^2\right)\left(m_e^2 M^2 - M^2 k\cdot k'\right.\right. \\ & +\; \left.\left. 2k\cdot pk'\cdot p\right)\right]\Bigg\}. \end{aligned} \tag{10.52}$$

Evaluating the kinematics in the Lab frame $k = (E, \vec{k})$, $p = (M, \vec{0})$, $k' = (E', \vec{k}')$, in the limit $m_e \to 0$ leads to the following relations

$$\begin{aligned} k\cdot p &= ME, \qquad\qquad k'\cdot p = ME', \\ k\cdot k' &= EE'(1-\cos\theta), \\ q^2 &= -2k\cdot k' = -2EE'(1-\cos\theta). \end{aligned}$$

Thus, Eq. (10.52) in the Lab frame is obtained as

$$\begin{aligned}\overline{\sum}\sum \mid \mathcal{M} \mid^2 \;=\; & \frac{8e^4}{q^4}\left\{ {F_M^p}^2(q^2)\left[ME\left\{ME' - \frac{q^2}{2}\right\} + ME'\left\{ME + \frac{q^2}{2}\right\} + M^2\frac{q^2}{2}\right]\right. \\ & -\; MF_M^p(q^2)\frac{F_2^p(q^2)}{2M}\left[2M^2q^2 + 8M^2EE'\right] \\ & +\; \left.\frac{{F_2^p}^2(q^2)}{4M^2}\left[\left\{2M^2 + ME - ME'\right\}\left\{M^2q^2 + 4M^2EE'\right\}\right]\right\}, \end{aligned} \tag{10.53}$$

and the differential scattering cross section is given by

$$\begin{aligned}\frac{d\sigma}{d\Omega} \;=\; & \frac{\alpha^2}{4\,E^2\sin^4\frac{\theta}{2}}\frac{E'}{E}\left\{\frac{(F_1^p(q^2) + \frac{q^2}{4M^2}F_2^p(q^2))^2 + \tau {F_M^p}^2(q^2)}{1+\tau}\cos^2\frac{\theta}{2}\right. \\ & +\; \left. 2\tau {F_M^p}^2(q^2)\sin^2\frac{\theta}{2}\right\}. \end{aligned} \tag{10.54}$$

Using $F_1^N(q^2), F_2^N(q^2)$ and $F_M^N(q^2)$ from Eqs. (10.48), (10.49) and (10.50), we obtain

$$\frac{d\sigma}{d\Omega} = \frac{\alpha^2}{4\,E^2\sin^4\frac{\theta}{2}}\frac{E'}{E}\left\{\frac{{G_E^p}^2(q^2) + \tau {G_M^p}^2(q^2)}{1+\tau}\cos^2\frac{\theta}{2} + 2\tau {G_M^p}^2(q^2)\sin^2\frac{\theta}{2}\right\}, \tag{10.55}$$

https://doi.org/10.1017/9781108489065.011 Published online by Cambridge University Press

Equation (10.55) is known as the Rosenbluth separation of the cross section for $e^- p$ scattering. The equation is used to experimentally determine the electric and magnetic form factors $G_E(q^2)$ and $G_M(q^2)$ as described in the next section.

Figure 10.8 presents the results for the differential scattering cross section $\frac{d\sigma}{d\Omega}$ vs. $\cos\theta$ for the elastic $e^- p$ scattering at different energies of the incoming electron viz. $E_e = 250$, 500, 750, and 1000 MeV. It may be observed that the differential scattering cross section is forward peaked and is similar to what we obtain in the case of $e^- \mu^-$ scattering.

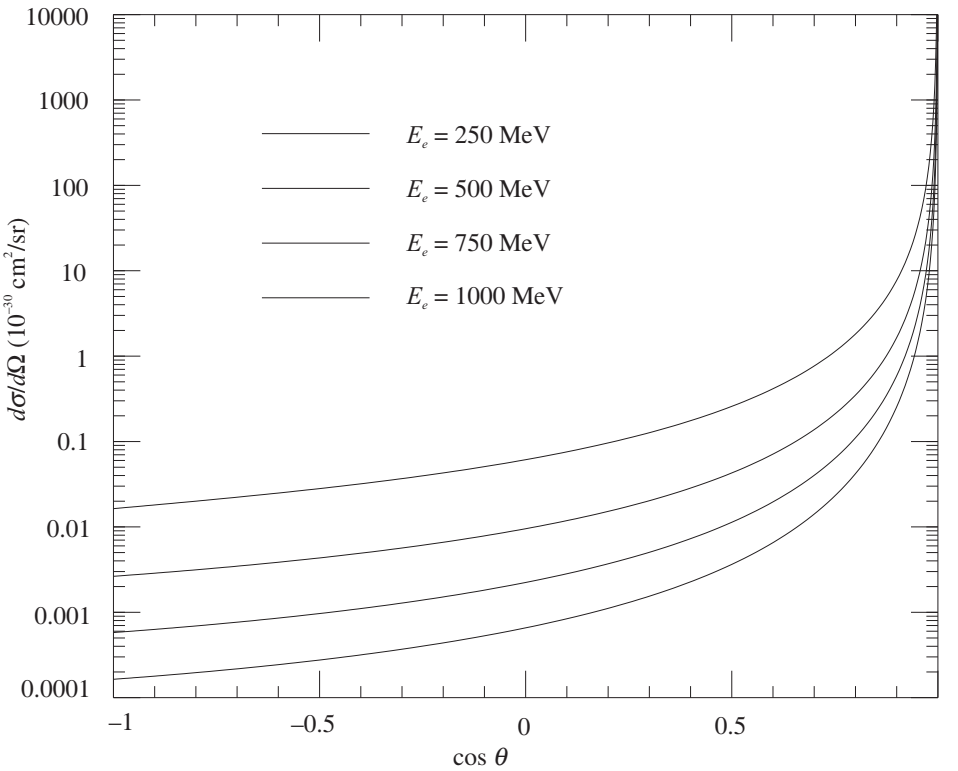

Figure 10.8 $\frac{d\sigma}{d\Omega}$ vs. $\cos\theta$ for the elastic $e^- p$ scattering at different incoming electron energies, viz., $E_e = 250$, 500, 750, and 1000 MeV.

10.4.4 Experimental determination of the form factors

Comparing Eqs. (10.55) and (10.13) (in the limit $E' = E$), one obtains

$$\left.\frac{d\sigma}{d\Omega}\right|_{\text{ep}} = \left.\frac{d\sigma}{d\Omega}\right|_{\text{Mott}} \left\{ \frac{G_E^{p\,2}(q^2) + \tau G_M^{p\,2}(q^2)}{1+\tau} + 2\tau G_M^{p\,2}(q^2) \tan^2\frac{\theta}{2} \right\}, \qquad (10.56)$$

where the quantity in the parentheses represents the structure of the nucleon.

https://doi.org/10.1017/9781108489065.011 Published online by Cambridge University Press

Equation (10.56) may be rewritten as

$$\frac{\frac{d\sigma}{d\Omega}\,|_{\rm ep}}{\frac{d\sigma}{d\Omega}\,|_{\rm Mott}} = \left\{\Phi(q^2) + \Psi(q^2)\,\tan^2\frac{\theta}{2}\right\}, \tag{10.57}$$

which is the equation of a straight line for a fixed q^2 with

$$\Phi(q^2) = \frac{G_E^{p\,2}(q^2) + \tau G_M^{p\;2}(q^2)}{1+\tau}, \qquad \Psi(q^2) = 2\tau G_M^{p\;2}(q^2),$$

as the intercept and slope, respectively, as shown in Figure 10.9. The experimental measurements for $e^- p$ elastic scattering have been performed and found to be consistent with the theoretical predictions.

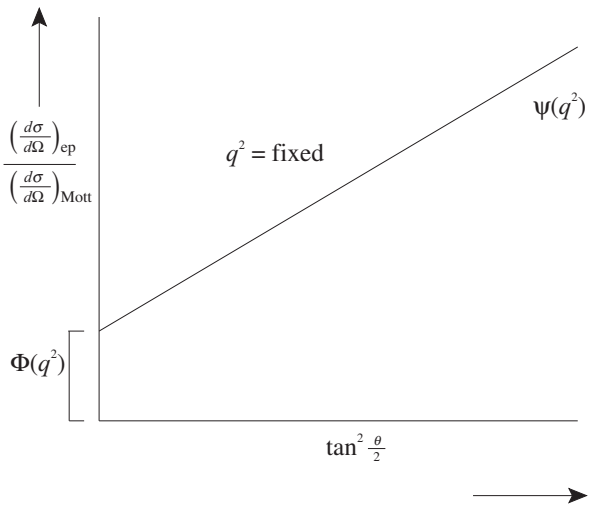

Figure 10.9 $\frac{\frac{d\sigma}{d\Omega}|_{\rm ep}}{\frac{d\sigma}{d\Omega}|_{\rm Mott}}$ vs. $\tan^2\frac{\theta}{2}$ for a fixed q^2.

The experimental values for the proton and neutron Sachs electric and magnetic form factors $G_E^{p,n}(q^2)$ and $G_M^{p,n}(q^2)$ at $q^2 = 0$ are given as

$$\begin{aligned} G_E^p(0) &= 1, & G_E^n(0) &= 0, \\ G_M^p(0) &= 2.7928\,\mu_N, & G_M^n(0) &= -1.913\,\mu_N, \end{aligned}$$

where μ_N is the nucleon magnetic moment. $G_E^{p,n}(0)$ gives the value of the electric charge for the proton and neutron. Similarly, $G_M^{p,n}(0)$ gives the magnetic moments of the proton and neutron. If the nucleons are assumed to be point particles, then the magnetic moments for the proton and neutron should be $G_M^p(0) = \mu_N$ and $G_M^n(0) = 0$. Therefore, the difference from μ_N in the case of the proton and from 0 in the case of the neutron represents the anomalous magnetic moments of the nucleons which provides evidence that nucleons are not point particles and have got structure.

https://doi.org/10.1017/9781108489065.011 Published online by Cambridge University Press

10.4.5 Numerical parameterization of the electromagnetic form factors

Initially, it was observed that the experimental data for the electromagnetic $e^- p$ scattering may be explained if one assumes the form factors to have a dipole form, that is,

$$G_E^p(q^2) = \frac{G_M^p(q^2)}{\mu_p} = \frac{G_M^n(q^2)}{\mu_n} = G_D(q^2), \tag{10.58}$$

where $G_D(q^2)$ is given as

$$G_D(q^2) = \frac{1}{\left(1 - \frac{q^2}{M_V^2}\right)^2}, \tag{10.59}$$

and M_V is known as the vector dipole mass. Initially, the best fit was found to be consistent with $M_V = 0.84$ GeV.

With the development of electron beam accelerators, many more measurements were performed like at MIT-Bates, MAMI, JLab, etc.; these measurements for the form factors found deviations from the dipole form. Figure 10.10 shows the deviation from a dipole form for the electric and magnetic form factors of nucleons. Therefore, there exist various parameterizations which show deviation from the dipole form like that of Galster et al. [414], which is given as

$$\begin{aligned} G_E^p(q^2) &= G_D(q^2), & G_M^p(q^2) &= (1+\mu_p) G_D(q^2), \\ G_M^n(q^2) &= \mu_n G_D(q^2), & G_E^n(q^2) &= \left(\frac{q^2}{4M^2}\right) \mu_n G_D(q^2) \xi_n, \\ \xi_n &= \frac{1}{\left(1 - \lambda_n \frac{q^2}{4M^2}\right)}, \end{aligned}$$

with $\mu_p = 1.7927 \mu_N$, $\mu_n = -1.913 \mu_N$, $M_V = 0.84$ GeV, and $\lambda_n = 5.6$.

Recently, several new parameterizations [415, 416, 417, 418] for the electromagnetic isovector form factors have been presented. In the following, we present the parameterizations given by Bradford et al. [416] known as BBBA-05 as well as the parameterization given by Kelly [417] and the modifications made by Punjabi et al. [418] in Kelly's parameterization for the electric and magnetic form factors of nucleons.

(i) **BBBA-05**

The expression for electric and magnetic Sachs form factor given by Bradford et al. [416] (BBBA-05) is

$$G_E^p(q^2) = \frac{1 - 0.0578\tau}{1 + 11.1\tau + 13.6\tau^2 + 33.0\tau^3},$$

https://doi.org/10.1017/9781108489065.011 Published online by Cambridge University Press

$$\frac{G_M^p(q^2)}{\mu_p} = \frac{1+0.15\tau}{1+11.1\tau+19.6\tau^2+7.54\tau^3},$$
$$G_E^n(q^2) = \frac{1.25\tau+1.30\tau^2}{1-9.86\tau+305\tau^2-758\tau^3+802\tau^4},$$
$$\frac{G_M^n(q^2)}{\mu_n} = \frac{1+1.81\tau}{1+14.1\tau+20.7\tau^2+68.7\tau^3}, \qquad \tau = -\frac{q^2}{4M^2}. \tag{10.60}$$

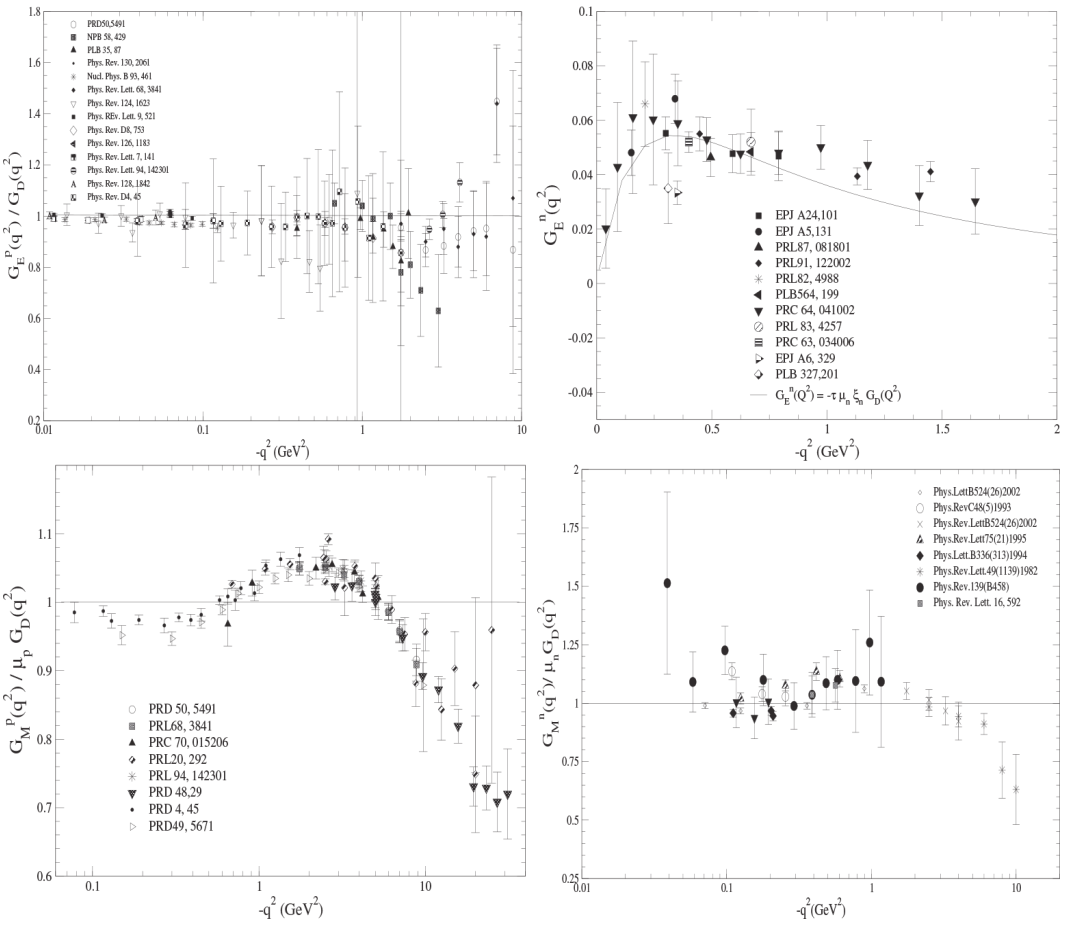

Figure 10.10 Experimental data for the electric and magnetic form factors for the proton.

(ii) **Kelly**
The parameterization for $G_E^{p,n}(q^2)$ and $G_M^{p,n}(q^2)$ given by Kelly [417] is

$$G_E^p(q^2) = \frac{1-0.24\tau}{1+10.98\tau+12.82\tau^2+21.97\tau^3},$$

https://doi.org/10.1017/9781108489065.011 Published online by Cambridge University Press

$$\begin{aligned}
\frac{G_M^p(q^2)}{\mu_p} &= \frac{1+0.12\tau}{1+10.97\tau+18.86\tau^2+6.55\tau^3}, \\
G_E^n(q^2) &= \frac{1.7\tau}{1+3.3\tau}\frac{1}{(1-q^2/(0.84)^2)^2}, \\
\frac{G_M^n(q^2)}{\mu_n} &= \frac{1+2.33\tau}{1+14.72\tau+24.20\tau^2+84.1\tau^3}.
\end{aligned} \tag{10.61}$$

(iii) **Punjabi et al.**
Punjabi et al. [418] have modified Kelly's fit [417] for G_E^n and G_E^p by including new data since the Kelly fit was done. Their best fits for $\mu_n G_E^n/G_M^n$ and $\mu_p G_E^p/G_M^p$ are given as:

$$\begin{aligned}
\frac{\mu_n G_E^n}{G_M^n} &= \frac{2.6316\tau}{1+4.118\sqrt{\tau}+0.29516\tau}, \\
\frac{\mu_p G_E^p}{G_M^p} &= \frac{1-5.7891\tau+14.493\tau^2-3.5032\tau^3}{1-5.5839\tau+12.909\tau^2+0.88996\tau^3+0.5420\tau^4}.
\end{aligned}$$

10.5 Quasielastic and Elastic ν Scattering Processes on Nucleons

10.5.1 Introduction

Neutrinos (ν_l) and antineutrinos ($\bar{\nu}_l$) interact with free nucleons via charged as well as neutral current induced weak processes. Here, we consider the neutrino and antineutrino induced charged current quasielastic and neutral current elastic interactions of the type

$$\left.\begin{aligned}
\nu_l(k) + n(p) &\to l^-(k') + p(p') \\
\bar{\nu}_l(k) + p(p) &\to l^+(k') + n(p')
\end{aligned}\right\} \quad \text{(Charged current)} \tag{10.62}$$

$$\left.\begin{aligned}
\nu_l(k) + n(p) &\to \nu_l(k') + n(p') \\
\nu_l(k) + p(p) &\to \nu_l(k') + p(p') \\
\bar{\nu}_l(k) + n(p) &\to \bar{\nu}_l(k') + n(p') \\
\bar{\nu}_l(k) + p(p) &\to \bar{\nu}_l(k') + p(p')
\end{aligned}\right\} \quad \text{(Neutral current)} \tag{10.63}$$

In these processes, k and k' are, respectively, the four momenta of the neutrino (antineutrino); the corresponding charged lepton and p and p' are the four momenta of the incoming and outgoing nucleons. Feynman diagrams corresponding to reactions given in Eqs. (10.62) and (10.63) are shown in Figure 10.11.

https://doi.org/10.1017/9781108489065.011 Published online by Cambridge University Press

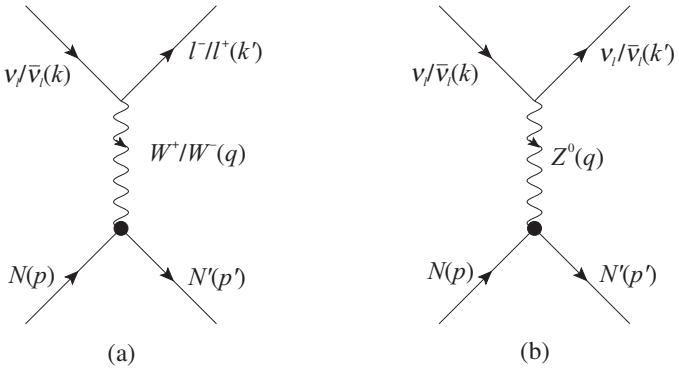

Figure 10.11 (a) Quasielastic and (b) Elastic ν scattering processes on nucleon ($N = n, p$ and $N' = p, n$) target.

10.5.2 Interaction Lagrangian

The interaction Lagrangian for the charged as well as the neutral current induced neutrino and antineutrino reactions on the free nucleon target in the standard model is written as (Chapter 8 for details)

$$\mathcal{L}_{\text{int}} = -\frac{g}{2\sqrt{2}} J_\mu^{CC} W^{+\mu} + \text{h.c} - \frac{g}{2\cos\theta_W} J_\mu^{NC} Z^\mu,$$

where the expression for the charged current is given by:

$$J_\mu^{CC} = \bar{\psi}'_q \gamma_\mu (1-\gamma_5) U_{\text{CKM}} \psi_q + \bar{\nu}_l \gamma_\mu (1-\gamma_5) l + \text{h.c.}$$

with $q' = (u, c, t)$, $q = (d, s, b)$. U_{CKM} is the CKM mixing matrix defined in Chapter 6.

The neutral current (NC) is given by:

$$J_\mu^{NC} = \Sigma_i \bar{\psi}_i \gamma_\mu (I_{3i} - Q_i \sin^2\theta_W) \psi_i,$$

where i runs over all the fermions of the standard model, that is, $\begin{pmatrix} \nu_l \\ l^- \end{pmatrix}_L$, ν_{lR}, l_R, $l = e, \mu, \tau$. I_3 is a weak isospin and Q is the charge of the ith fermion as well as for all the quark flavors.

At the nucleon level in the limit $M_W^2, M_Z^2 >> q^2$, the Lagrangian for the charged current (CC) reaction is expressed as:

$$\mathcal{L}_{\text{int}} = -\frac{G_F}{\sqrt{2}} a J_\mu^h l^\mu + \text{h.c.}$$

with

$$\begin{aligned}
J_\mu^h &= V_\mu^{1+i2} - A_\mu^{1+i2} \quad \text{and} \quad a = \cos\theta_c \quad \text{for } \Delta S = 0 \text{ CC reactions,} \\
J_\mu^h &= V_\mu^{4+i5} - A_\mu^{4+i5} \quad \text{and} \quad a = \sin\theta_c \quad \text{for } \Delta S = 1 \text{ CC reactions, and} \\
J_\mu^h &= V_\mu^{NC} - A_\mu^{NC} \quad \text{and} \quad a = 1 \quad \text{for the } \Delta S = 0 \text{ NC reactions}
\end{aligned}$$

https://doi.org/10.1017/9781108489065.011 Published online by Cambridge University Press

where

$$V_\mu^{NC} = V_\mu^3 - 2\sin^2\theta_W J_\mu^{\rm em} - \frac{1}{2}(V_\mu^S - A_\mu^S),$$
$$A_\mu^{NC} = A_\mu^3 - \frac{1}{2}A_\mu^S.$$

In this expression, the superscript i in V_μ^i and A_μ^i refers to the SU(3) index and are discussed in Chapter 8. S refers to the strangeness current which are isoscalar.

10.5.3 Charged current quasielastic reaction and weak nucleon form factors

In a charged current reaction, the basic reaction (Figure 10.11(a)) for the quasielastic scattering process is a neutrino (antineutrino) interacting with a free neutron (proton). It is given by

$$\nu_l(k) + n(p) \longrightarrow l^-(k') + p(p'), \tag{10.64}$$
$$\bar{\nu}_l(k) + p(p) \longrightarrow l^+(k') + n(p'), \qquad l = e, \mu, \tau. \tag{10.65}$$

The invariant matrix element for the charged current quasielastic reaction of a neutrino and an antineutrino with a nucleon, given by Eqs. (10.64) and (10.65), is written as

$$\mathcal{M} = \frac{G_F}{\sqrt{2}}\cos\theta_C\, l_\mu\, J^\mu, \tag{10.66}$$

where G_F is the Fermi coupling constant, θ_C is the Cabibbo angle, and the leptonic weak current is given by

$$l_\mu = \bar{u}(\vec{k}')\gamma_\mu(1 \mp \gamma_5)u(\vec{k}). \tag{10.67}$$

$-(+)$ shows that it is a neutrino (antineutrino) induced quasielastic scattering process. The hadronic current J^μ is given by

$$J_\mu = \bar{u}(\vec{p}\,')\Gamma_\mu u(\vec{p}) \tag{10.68}$$

with

$$\Gamma_\mu = V_\mu - A_\mu. \tag{10.69}$$

The matrix elements of the vector (V_μ) and the axial vector (A_μ) currents are given by:

$$\langle N'(\vec{p}\,')|V_\mu|N(\vec{p})\rangle = \bar{u}(\vec{p}\,')\left[\gamma_\mu f_1(q^2) + i\sigma_{\mu\nu}\frac{q^\nu}{(M+M')}f_2(q^2) + \frac{2q_\mu}{(M+M')}f_3(q^2)\right]u(\vec{p}), \tag{10.70}$$

https://doi.org/10.1017/9781108489065.011 Published online by Cambridge University Press

$$\begin{aligned}\langle N'(\vec{p}\,')|A_\mu|N(\vec{p})\rangle &= \bar{u}(\vec{p}\,')\left[\gamma_\mu\gamma_5 g_1(q^2) + i\sigma_{\mu\nu}\frac{q^\nu}{(M+M')}\gamma_5 g_2(q^2)\right.\\ &+ \left.\frac{2q_\mu}{(M+M')}\gamma_5 g_3(q^2)\right]u(\vec{p}), \end{aligned} \tag{10.71}$$

where $N, N' = n, p$, $q^2 = (k-k')^2$ is the four momentum transfer squared. M and M' are the masses of the initial and the final nucleon, respectively. $f_1(q^2)$, $f_2(q^2)$, and $f_3(q^2)$ are the vector, weak magnetic, and induced scalar form factors and $g_1(q^2)$, $g_2(q^2)$, and $g_3(q^2)$ are the axial vector, induced tensor (or weak electric), and induced pseudoscalar form factors, respectively. The details about these form factors are discussed in Chapter 6.

Using the leptonic and hadronic currents given in Eqs. (10.67) and (10.68) in Eq. (10.66), the matrix element squared is obtained as

$$|\mathcal{M}|^2 = \frac{G_F^2}{2}\cos^2\theta_C\, L^{\mu\nu}J_{\mu\nu}. \tag{10.72}$$

The leptonic tensor $L^{\mu\nu}$ is calculated to be (Appendix D)

$$L^{\mu\nu} = 8\left[k^\mu k'^\nu + k'^\mu k^\nu - g^{\mu\nu}\, k\cdot k' \pm i\epsilon^{\mu\nu\alpha\beta}\, k'_\alpha k_\beta\right]. \tag{10.73}$$

$+(-)$ shows that it is a neutrino (antineutrino) induced process.

The hadronic tensor $J_{\mu\nu}$ given in Eq. (10.72), is obtained using Eq. (10.68) averaged over the initial spin state of the nucleon and summed over the final spin state as:

$$\begin{aligned} J_{\mu\nu} &= \overline{\sum}\sum J_\mu^\dagger J_\nu \\ &= \frac{1}{2}\mathrm{Tr}\left[(\not{p}' + M)\Gamma_\mu(\not{p} + M)\tilde{\Gamma}_\nu\right], \end{aligned} \tag{10.74}$$

where

$$\begin{aligned}\Gamma_\mu &= \left[f_1(q^2)\gamma_\mu + i\sigma_{\mu\nu}\frac{q^\nu}{(M+M')}f_2(q^2) + \frac{2q_\mu}{(M+M')}f_3(q^2) - g_1(q^2)\gamma_\mu\gamma_5\right.\\ &- \left. i\sigma_{\mu\nu}\frac{q^\nu}{(M+M')}\gamma_5 g_2(q^2) - \frac{2q_\mu}{(M+M')}\gamma_5 g_3(q^2)\right], \end{aligned} \tag{10.75}$$

and $\tilde{\Gamma}_\nu = \gamma^0\,{\Gamma_\nu}^\dagger\,\gamma^0$. Using Eq. (10.75) in Eq. (10.74), we obtain $J_{\mu\nu}$ as

$$\begin{aligned} J_{\mu\nu} &= \frac{1}{2}\left[4f_1^2(q^2)\left(p'_\mu p_\nu + p'_\nu p_\mu - (p\cdot p' - MM')g_{\mu\nu}\right)\right.\\ &+ 4\frac{f_2^2(q^2)}{(M+M')^2}\left(MM'q^2 g_{\mu\nu} + q_\mu\left(-q_\nu(MM' + p\cdot p') + p'_\nu p\cdot q + p_\nu p'\cdot q\right)\right.\\ &- \left. 2g_{\mu\nu}p\cdot q p'\cdot q + q^2 g_{\mu\nu}p\cdot p' - q^2 p_\mu p'_\nu + p_\mu q_\nu p'\cdot q + p'_\mu\left(q_\nu p\cdot q - q^2 p_\nu\right)\right)\\ &+ \frac{16f_3^2(q^2)}{(M+M')^2}\left(q_\mu q_\nu(MM' + p\cdot p')\right) + 4g_1^2(q^2)\left((p'_\mu p_\nu + p_\mu p'_\nu) - (p\cdot p' + MM')g_{\mu\nu}\right)\\ &+ \left.\frac{4g_2^2(q^2)}{(M+M')^2}\left(-MM'q^2 g_{\mu\nu} + q_\mu\left(q_\nu(MM' - p\cdot p') + p'_\nu p\cdot q + p_\nu p'\cdot q\right)\right.\right. \end{aligned}$$

https://doi.org/10.1017/9781108489065.011 Published online by Cambridge University Press

$$
\begin{aligned}
&- \quad 2g_{\mu\nu}p\cdot qp'\cdot q + q^2 g_{\mu\nu}p\cdot p' - q^2 p_\mu p'_\nu + p_\mu q_\nu p'\cdot q + p'_\mu\left(q_\nu p\cdot q - q^2 p_\nu\right)\Big)\\
&+ \quad \frac{16g_3^2(q^2)}{(M+M')^2}\left(q_\mu q_\nu(p'\cdot p - MM')\right)\\
&+ \quad \frac{4f_1(q^2)f_2(q^2)}{(M+M')}\left(q_\mu\left(M'p_\nu - Mp'_\nu\right) + 2Mg_{\mu\nu}p'\cdot q - Mp'_\mu q_\nu - 2M'g_{\mu\nu}p\cdot q + M'p_\mu q_\nu\right)\\
&+ \quad \frac{8f_1(q^2)f_3(q^2)}{(M+M')}\left(q_\mu\left(Mp'_\nu + M'p_\nu\right) + q_\nu\left(Mp'_\mu + M'p_\mu\right)\right) + 8if_1(q^2)g_1(q^2)\left(\epsilon_{\mu\nu\alpha\beta}\,p^\alpha p'^\beta\right)\\
&+ \quad \frac{8if_1(q^2)g_2(q^2)}{(M+M')}\left(M'\epsilon_{\mu\nu\alpha\beta}p^\alpha q^\beta - M\epsilon_{\mu\nu\alpha\beta}p'^\alpha q^\beta\right) + \frac{8f_2(q^2)f_3(q^2)}{(M+M')^2}\left(q_\nu\left(p_\mu p'\cdot q - p'_\mu p\cdot q\right)\right.\\
&+ \quad \left.q_\mu\left(p_\nu p'\cdot q - p'_\nu p\cdot q\right)\right) + 8i\left(\frac{f_2(q^2)g_1(q^2)}{(M+M')}\right)\left(M\epsilon_{\mu\nu\alpha\beta}p'^\alpha q^\beta + M'\epsilon_{\mu\nu\alpha\beta}p^\alpha q^\beta\right)\\
&+ \quad \frac{8if_2(q^2)g_2(q^2)}{(M+M')^2}\left(q_\mu\epsilon_{\nu\alpha\beta\delta}p^\alpha p'^\beta q^\delta - q_\nu\epsilon_{\mu\alpha\beta\delta}p^\alpha p'^\beta q^\delta + q^2\epsilon^{\mu\nu\alpha\beta}p^\alpha p'^\beta + 2p\cdot q\epsilon^{\mu\nu\alpha\beta}p'^\alpha q^\beta\right)\\
&+ \quad \frac{8if_2(q^2)g_3(q^2)}{(M+M')^2}\left(q_\mu\epsilon_{\nu\alpha\beta\delta}p^\alpha p'^\beta q^\delta - q_\nu\epsilon_{\mu\alpha\beta\delta}p^\alpha p'^\beta q^\delta\right)\\
&+ \quad \frac{8if_3(q^2)g_2(q^2)}{(M+M')^2}\left(q_\mu\epsilon_{\nu\alpha\beta\delta}p^\alpha p'^\beta q^\delta - q_\nu\epsilon_{\mu\alpha\beta\delta}p^\alpha p'^\beta q^\delta\right)\\
&+ \quad \frac{4g_1(q^2)g_2(q^2)}{(M+M')}\left(q_\mu\left(Mp'_\nu + M'p_\nu\right) - 2Mg_{\mu\nu}p'\cdot q + Mp'_\mu q_\nu - 2M'g_{\mu\nu}p\cdot q + M'p_\mu q_\nu\right)\\
&+ \quad \frac{8g_1(q^2)g_3(q^2)}{(M+M')}\left(q_\mu\left(M'p_\nu - Mp'_\nu\right) + q_\nu\left(M'p_\mu - Mp'_\mu\right)\right)\\
&+ \quad \frac{8g_2(q^2)g_3(q^2)}{(M+M')^2}\left(q_\nu\left(p_\mu p'\cdot q - p'_\mu p\cdot q\right) + q_\mu\left(p_\nu p'\cdot q - p'_\nu p\cdot q\right)\right)\Bigg]. \qquad (10.76)
\end{aligned}
$$

Contraction of the various terms of the hadronic tensor $J_{\mu\nu}$ with the leptonic tensor $L^{\mu\nu}$ yields

$$|\mathcal{M}|^2 = \frac{G_F^2}{2}\cos^2\theta_c N(q^2), \qquad (10.77)$$

where $N(q^2) = L^{\mu\nu}J_{\mu\nu}$ and is given in Appendix F. Using the general expression for the differential scattering cross section in the Lab frame (Figure 10.12), we obtain

$$\frac{d\sigma}{dq^2} = \frac{G_F^2\cos^2\theta_c}{8\pi M^2 E_{\nu(\bar{\nu})}^2}N(q^2), \qquad (10.78)$$

where $E_{\nu(\bar{\nu})}$ is the energy of the incoming (anti)neutrino.

The differential scattering cross section may also be expressed in terms of the Mandelstam variables s, t, u as:

$$\frac{d\sigma}{dq^2} = \frac{G_F^2M^2\cos^2\theta_C}{8\pi E_\nu^2}\left[A(q^2) \mp B(q^2)\,\frac{(s-u)}{M^2} + C(q^2)\,\frac{(s-u)^2}{M^4}\right]. \qquad (10.79)$$

The negative (positive) sign before the $B(q^2)$ term refers to neutrino (antineutrino) scattering. The following assumptions have been taken into account while obtaining the expression in

https://doi.org/10.1017/9781108489065.011 Published online by Cambridge University Press

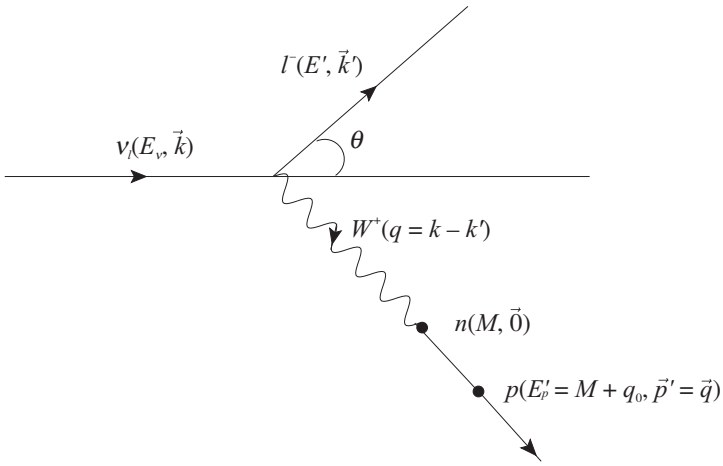

Figure 10.12 Kinematics in the Lab frame showing $\nu_l + n \to l^- + p$ scattering process.

Eq. (10.79): $M' = M$, $s - u = 4ME_\nu + q^2$ and there are no second class currents, that is, $f_3(q^2) = g_2(q^2) = 0$.

The factors $A(q^2)$, $B(q^2)$, and $C(q^2)$ are given as:

$$A(q^2) = \frac{m^2 - q^2}{4M^2}\left[\left(4 - \frac{q^2}{M^2}\right)g_1^2(q^2) - \left(4 + \frac{q^2}{M^2}\right)f_1^2(q^2) - \frac{q^2}{M^2}\left(1 + \frac{q^2}{4M^2}\right)f_2^2(q^2)\right.$$
$$- \frac{4q^2}{M^2}f_1(q^2)f_2(q^2) - \frac{m_l^2}{M^2}\left(\left(f_1(q^2) + f_2(q^2)\right)^2 + \left(g_1(q^2) + 2g_3(q^2)\right)^2\right.$$
$$\left.\left. + \left(\frac{q^2}{M^2} - 4\right)g_3^2(q^2)\right)\right], \tag{10.80}$$

$$B(q^2) = -\frac{q^2}{M^2}g_1^2(q^2)\left[f_1(q^2) + f_2(q^2)\right], \tag{10.81}$$

$$C(q^2) = \frac{1}{4}\left[g_1^2(q^2) + (f_1(q^2))^2 - \frac{q^2}{4M^2}(f_2(q^2))^2\right]. \tag{10.82}$$

The parameterizations for $f_i(q^2)$ and $g_i(q^2)$ are given in Section 10.5.6.

10.5.4 Neutral current elastic reactions and weak nucleon form factors

We first define the matrix elements for the neutral current processes on the proton and the neutron targets, that is,

$$\nu_l(k) + p(p) \longrightarrow \nu_l(k') + p(p'),$$
$$\nu_l(k) + n(p) \longrightarrow \nu_l(k') + n(p'),$$

https://doi.org/10.1017/9781108489065.011 Published online by Cambridge University Press

in terms of the neutral current form factors $\tilde{f}_i^{p,n}(q^2)$ and $\tilde{g}_i^{p,n}(q^2)(i = 1,2,3)$ for the protons and neutrons, respectively, as

$$\begin{aligned}\left\langle \vec{p}\,' \mid J_\mu^{NC} \mid \vec{p} \right\rangle_p &= \bar{u}(\vec{p}\,') \left[\gamma_\mu \tilde{f}_1^p(q^2) + \frac{i\sigma_{\mu\nu}q^\nu \tilde{f}_2^p(q^2)}{2M} + \frac{q_\mu}{M}\gamma_5 \tilde{f}_3^p(q^2) \right. \\ &\quad \left. + \gamma_\mu\gamma_5 \tilde{g}_1^p(q^2) + \frac{(p_\mu + p'_\mu)}{M}\gamma_5 \tilde{g}_2^p(q^2) + \frac{q_\mu \gamma_5 \tilde{g}_3^p(q^2)}{M} \right] u(\vec{p}), \\ \left\langle \vec{p}\,' \mid J_\mu^{NC} \mid \vec{p} \right\rangle_n &= \bar{u}(\vec{p}\,') \left[\gamma_\mu \tilde{f}_1^n(q^2) + \frac{i\sigma_{\mu\nu}q^\nu \tilde{f}_2^n(q^2)}{2M} + \frac{q_\mu}{M}\gamma_5 \tilde{f}_3^n(q^2) \right. \\ &\quad \left. + \gamma_\mu\gamma_5 \tilde{g}_1^n(q^2) + \frac{(p_\mu + p'_\mu)}{M}\gamma_5 \tilde{g}_2^n(q^2) + \frac{q_\mu \gamma_5 \tilde{g}_3^n(q^2)}{M} \right] u(\vec{p}),\end{aligned}$$

where $\tilde{f}_1(q^2)$, $\tilde{f}_2(q^2)$, $\tilde{g}_1(q^2)$, and $\tilde{g}_3(q^2)$ are known as the first class neutral current form factors while $\tilde{f}_3(q^2)$ and $\tilde{g}_2(q^2)$ are known as the second class form factors. The parameterizations for $\tilde{f}_i(q^2)$ and $\tilde{g}_i(q^2)$ are given in Section 10.5.6.

10.5.5 Symmetry properties of weak hadronic currents and form factors

The weak form factors are constrained by the following symmetry properties of the weak hadronic currents:

(a) T invariance implies that all the form factors $f_{1-3}(q^2)$ and $g_{1-3}(q^2)$ are real.

(b) The assumption that the charged weak vector current and its conjugate along with the isovector part of the electromagnetic current form an isotriplet implies that the charged weak vector form factors $f_1(q^2)$ and $f_2(q^2)$ are related to the isovector electromagnetic form factors of the nucleon.

(c) The principle of conserved vector current (CVC) of weak vector currents implies that $f_3(q^2) = 0$.

(d) The principle of G-invariance implies that $f_3(q^2) = 0$ and $g_2(q^2) = 0$.

(e) The hypothesis of the partially conserved axial vector current (PCAC) relates $g_3(q^2)$ to $g_1(q^2)$ through the Goldberger–Treiman (GT) relation.

The implications of these symmetry properties have already been discussed in Chapter 6.

10.5.6 Parameterization of the weak form factors

(i) Vector form factors

In the case of charged current interactions, the hadronic current contains two isovector form factors $f_{1,2}(q^2)$ of the nucleons, which can be related to the isovector combination of the Dirac-Pauli form factors $F_{1,2}^p(q^2)$ and $F_{1,2}^n(q^2)$ of the proton and the neutron using the relation

https://doi.org/10.1017/9781108489065.011 Published online by Cambridge University Press

$$f_{1,2}(q^2) = F^p_{1,2}(q^2) - F^n_{1,2}(q^2). \tag{10.83}$$

The Dirac and Pauli form factors are, in turn, expressed in terms of the experimentally determined Sachs electric and magnetic form factors as discussed in Section 10.4 (Eqs. (10.46) and (10.47)).

The vector form factors for the neutral current induced processes are obtained as

$$\tilde{f}^p_{1,2}(q^2) = \left(\frac{1}{2} - 2\sin^2\theta_W\right) F^p_{1,2}(q^2) - \frac{1}{2}F^n_{1,2}(q^2) - \frac{1}{2}F^s_{1,2}(q^2), \tag{10.84}$$

$$\tilde{f}^n_{1,2}(q^2) = \left(\frac{1}{2} - 2\sin^2\theta_W\right) F^n_{1,2}(q^2) - \frac{1}{2}F^p_{1,2}(q^2) - \frac{1}{2}F^s_{1,2}(q^2), \tag{10.85}$$

where θ_W is the Weinberg angle, and $F^s_1(q^2)$ and $F^s_2(q^2)$ are the strangeness vector form factors, which are discussed in this Section under the heading Strangeness form factors..

(ii) Axial vector form factor

The isovector axial vector form factor is parameterized as

$$g_1(q^2) = g_A(0)\left[1 - \frac{q^2}{M_A^2}\right]^{-2}, \tag{10.86}$$

where $g_A(0)(= C_A)$ is determined experimentally from the β-decay of neutrons as discussed in Chapter 5. M_A is known as the axial dipole mass and is obtained from the quasielastic neutrino and antineutrino scattering as well as from pion electroproduction data (Figure 10.13). The dipole parameterization is extensively used in the analysis of various experiments in quasielastic scattering. However, recently a new parameterization based on Z-expansion has been proposed in literature [419, 420]. Theoretically, $g_1(q^2)$ is calculated in various models of lattice gauge theory [419, 421, 422, 423, 424] and quark models [425].

The numerical value of M_A to be used in the calculations of neutrino–nucleon cross section is a subject of intense discussion in the neutrino physics community and a wide range of M_A have been recently discussed in the literature [356, 426, 427]. The old data available on (anti)neutrino scattering on hydrogen and deuterium targets [428, 429, 430] reanalyzed by Bodek et al. [431] gives a value of $M_A = 1.014 \pm 0.014$ GeV, while a recent analysis of the same data by Meyer et al. [420] gives a value in the range of 1.02–1.17 GeV depending upon which, data of ANL [428], BNL [429], and FNAL [430] experiments are considered. In 2002, Bernard et al. have reanalyzed the data of the neutrino and antineutrino scattering on hydrogen and deuterium targets as well as the electroproduction data and got the best χ^2 fit for M_A as:

$$M_A = 1.026 \pm 0.021 \text{ GeV}.$$

In recent years, high statistics data on quasielastic neutrino–nucleus scattering have been obtained and analyzed from neutrino and antineutrino scattering on nuclear targets both at low and intermediate energies. The data from NOMAD [432], MINERνA [433] favor a lower value

https://doi.org/10.1017/9781108489065.011 Published online by Cambridge University Press

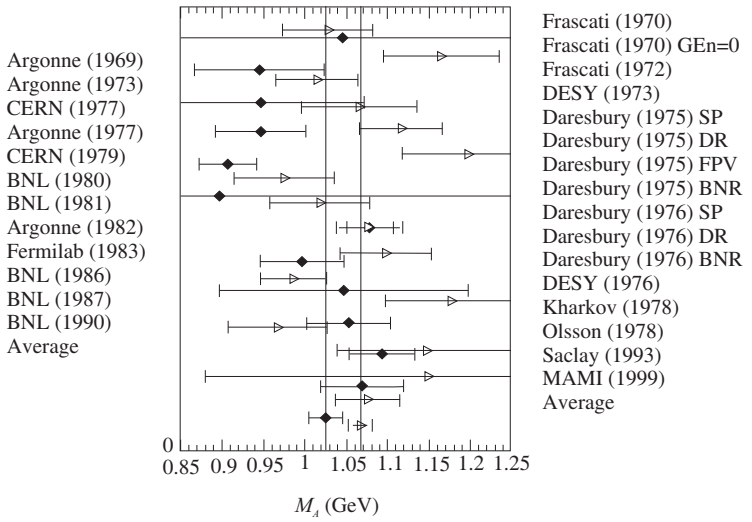

Figure 10.13 Axial mass M_A extractions from (quasi)elastic neutrino and antineutrino scattering experiments on hydrogen and deuterium targets (diamond) and from charged pion electroproduction experiments (triangle). The weighted average from the neutrino/antineutrino experiments is $M_A = 1.026 \pm 0.021$ GeV and from the electroproduction experiments is $M_A = 1.069 \pm 0.016$ GeV.

of M_A, around 1.03 GeV, while the data from MiniBooNE [434, 353, 435], MINOS [436, 437], K2K [438], T2K [439], and SciBooNE [440, 441] favor a higher value of M_A which lies in the range of 1.2–1.35 GeV. The recently suggested values of M_A from these experiments have been tabulated in Table 10.1. We shall discuss these experiments and the values of M_A determined from them alongwith the role of nuclear medium effects in Chapter 14.

In the case of neutral current induced reactions, the axial vector form factor for the nucleon is given by:

$$\tilde{g}^1_{p,n}(q^2) = \pm\frac{1}{2}g_1(q^2) - \frac{1}{2}F^s_A(q^2), \tag{10.87}$$

where $g_1(q^2)$ is given in Eq. (10.86) with $M_A = 1.026$ GeV. $F^s_A(q^2)$ is the strangeness axial vector form factor.

Table 10.1 Recent measurements of the axial dipole mass (M_A).

Experiment	M_A (GeV)	Experiment	M_A (GeV)
MINERνA [433, 442]	0.99	SciBooNE [440]	1.21±0.22
NOMAD [432]	1.05±0.02±0.06	K2K-SciBar [438]	1.144±0.077
MiniBooNE [434, 353, 435]	1.23±0.20	K2K-SciFi [438]	1.20±0.12
MINOS [436, 437]	1.19($Q^2 > 0$) 1.26($Q^2 > 0.3$ GeV^2)	World Average	1.026± 0.021 [443] 1.014±0.014 [431]

https://doi.org/10.1017/9781108489065.011 Published online by Cambridge University Press

(iii) Pseudoscalar form factor

In the charged current sector, the pseudoscalar form factor $g_3(q^2)$ is dominated by the pion pole. It is given in terms of the Goldberger–Treiman relation near $q^2 \approx 0$ if PCAC is assumed and is related to the axial vector form factor $g_1(q^2)$ as

$$g_3(q^2) = \frac{2M^2 g_1(q^2)}{m_\pi^2 - q^2}. \tag{10.88}$$

However, in the literature, there are other versions of the pseudoscalar form factor like [444]:

$$g_3(Q^2) \;=\; -\frac{M}{q^2}\left[\left(\frac{2m_\pi^2 f_\pi}{m_\pi^2 - q^2}\right)\left(\frac{Mg_A(0)}{f_\pi} - \frac{g_{\pi NN}(0)\Delta q^2}{m_\pi^2}\right) + 2Mg_1(q^2)\right], \tag{10.89}$$

where $g_{\pi NN}(0) = 13.21$, $f_\pi = 92.42$ MeV, and $\Delta = 1 + \frac{Mg_A(0)}{f_\pi g_{\pi NN}(0)}$.

ahe pseudoscalar form factor using chiral perturbation theory (ChPT) is given by [444, 445]

$$g_3(0) = \frac{2Mg_{\pi NN}(0) f_\pi}{m_\pi^2 - q^2} + \frac{g_A(0) M^2 r_A^2}{3}, \tag{10.90}$$

where axial radius $r_A = \frac{2\sqrt{3}}{M_A}$. There are many more.

The contribution from the pseudoscalar form factor is proportional to the mass of the lepton and hence, in the case of neutral current reactions, it vanishes.

(iv) Second class current form factors

In the $\Delta S = 0$ sector, the violation of G-parity due to difference in mass of u and d quarks or the intrinsic charge symmetry violation of the strong interaction is very small. The form factors $f_3(q^2)$ and $g_2(q^2)$ are expected to be very small too. Moreover, in the vector sector, the charged weak vector currents V_μ along with the isovector part of the electromagnetic current ($J_\mu^{\rm em}$) is assumed to form an isotriplet, which leads to the hypothesis of CVC and predicts $f_3(q^2) = 0$. However, in the axial vector sector, there is no such constraint on the form factor $g_2(q^2)$ and it could be nonvanishing albeit small. It is because of this reason that most of the experiments in the $\Delta S = 0$ sector are analyzed for the search of the second class current (SCC) assuming $f_3(q^2) = 0$ with a nonvanishing $g_2(q^2)$ which is found to be small. Generally, the form factor $g_2(q^2)$, in analogy with $g_1(q^2)$, is expressed as

$$g_2(q^2) = g_2(0)\left[1 - \frac{q^2}{M_2^2}\right]^{-2}, \tag{10.91}$$

where for simplicity, $M_2 = M_A$.

This form factor $g_2(q^2)$ may also give information about the time reversal invariance (TRI). If TRI is assumed, then all the form factors must be real; in the absence of TRI, the form factor

https://doi.org/10.1017/9781108489065.011 Published online by Cambridge University Press

$g_2(q^2)$ can be taken as imaginary. We have explored the possibility of both real and imaginary $g_2(q^2)$, which are represented later in the text as $g_2^R(q^2)$ and $g_2^I(q^2)$, respectively.

(v) Strangeness form factors

The strangeness vector form factors $F_1^s(q^2)$ and $F_2^s(q^2)$ may be redefined in terms of the strangeness Sachs electric and magnetic form factors as:

$$G_E^s(q^2) = F_1^s(q^2) - \tau F_2^s(q^2), \tag{10.92}$$

$$G_M^s(q^2) = F_1^s(q^2) + F_2^s(q^2). \tag{10.93}$$

At $q^2 = 0$, the Sachs electric form factor gives the net strangeness of the nucleon, that is, $G_E^s(0) = 0$. At low momentum transfer, the electric form factor is expressed in terms of ρ^s, that is,

$$\rho^s = \frac{dG_E^s(q^2)}{dq^2} = -\frac{1}{6}\langle r_s^2\rangle, \tag{10.94}$$

where $\langle r_s^2\rangle$ is the strangeness radius. Similarly, at $q^2 = 0$, $G_M^s(q^2) = \mu^s$, the strangeness magnetic moment. Therefore, these two parameters ρ^s and μ^s determine the neutral current form factors $F_1^s(q^2)$ and $F_2^s(q^2)$. The q^2 dependence of $G_E^s(q^2)$ and $G_M^s(q^2)$ are obtained as:

$$G_E^s = \frac{\rho^s\tau}{\left(1 - \frac{q^2}{\Lambda_E^2}\right)}, \qquad G_M^s = \frac{\mu^s}{\left(1 - \frac{q^2}{\Lambda_M^2}\right)}, \tag{10.95}$$

where one of the fits [446] for ρ^s and μ^s assuming $\Lambda_{E,M}^s$ to be very large, gives

$$\rho^s = 0.13 \pm 0.21 \qquad \text{and} \qquad \mu^s = 0.035 \pm 0.053.$$

The strangeness axial vector form factor $F_A^s(q^2)$ is taken to be of dipole form:

$$F_A^s(q^2) = \frac{\Delta s}{\left(1 - \frac{q^2}{M_A^2}\right)^2}, \tag{10.96}$$

where Δs is the strange quark contribution to the nucleon spin and is determined from the neutral current neutrino scattering and scattering of polarized electrons from nucleons [447, 353].

10.5.7 Cross sections for charged current processes

Figure 10.14 presents the results for the differential scattering cross section $\frac{d\sigma}{dq^2}$ vs. $-q^2$, for the neutrino as well as antineutrino induced quasielastic processes, that is, $\nu_\mu + n \to \mu^- + p$ and $\bar{\nu}_\mu + p \to \mu^+ + n$, at the two values of incoming (anti)neutrino energies, viz., $E_{\nu_\mu(\bar{\nu}_\mu)} =$ 500 MeV and 1 GeV. Moreover, we have presented the results for two different values of the axial dipole mass, viz., $M_A = 1.026$ and 1.2 GeV. It may be noticed that with the increase in

https://doi.org/10.1017/9781108489065.011 Published online by Cambridge University Press

the value of M_A, the differential scattering cross section increases. In the case of the neutrino induced process, 20% increase in the value of M_A, increases the cross section by about 20%; in the case of the antineutrino induced process, 20% increase in the value of M_A results in an increment in the cross section by about 5%.

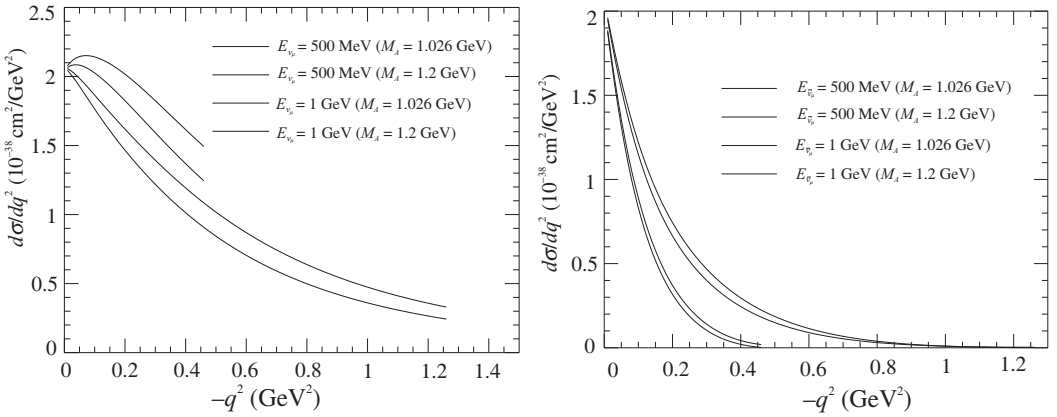

Figure 10.14 $\frac{d\sigma}{dq^2}$ vs. $-q^2$ for the $\nu_\mu + n \to \mu^- + p$ (left panel) and $\bar{\nu}_\mu + p \to \mu^+ + n$ (right panel) at the different (anti)neutrino energies, viz., $E_{\nu_\mu(\bar{\nu}_\mu)}$ = 500 MeV and 1 GeV and at $M_A = 1.026$ and 1.2 GeV.

In Figure 10.15, the results for the total scattering cross section as a function of incoming (anti)neutrino energy are presented for the processes $\nu_l + n \to l^- + p$ and $\bar{\nu}_l + p \to l^+ + n$ with $l = e, \mu$ at $M_A = 1.026$ and 1.2 GeV. It may be observed that at low (anti)neutrino energies $< (0.3)0.8$ GeV, the cross section for ν_e $(\bar{\nu}_e)$ is larger than the cross section for ν_μ $(\bar{\nu}_\mu)$, which is basically a threshold effect. However, with increase in energy, that is, $E_{\nu_l(\bar{\nu}_l)} > 0.8(0.3)$ GeV, the cross sections for ν_e $(\bar{\nu}_e)$ and ν_μ $(\bar{\nu}_\mu)$ are almost comparable.

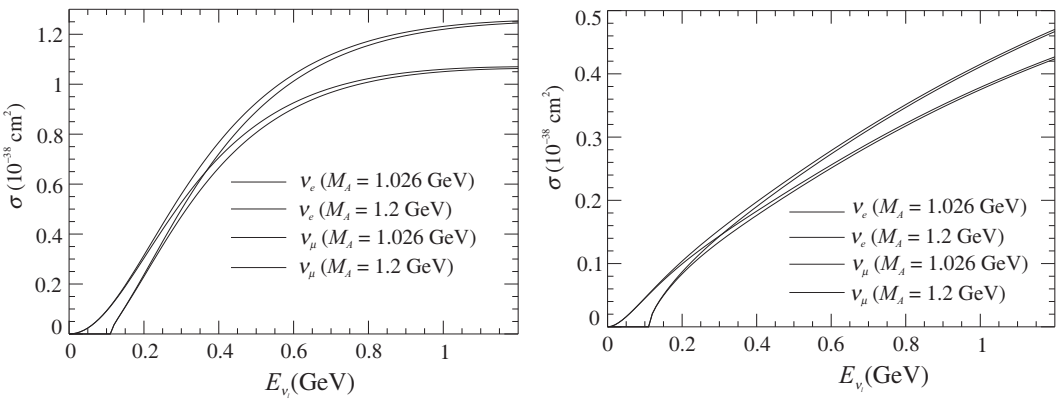

Figure 10.15 σ vs. $E_{\nu_l(\bar{\nu}_l)}$ for the $\nu_l + n \to l^- + p$ (left panel) and $\bar{\nu}_l + p \to l^+ + n$ (right panel) with $l = e, \mu$ at $M_A = 1.026$ and 1.2 GeV.

In Figure 10.16, we show the dependence of the total scattering cross section on M_A with or without the presence of $g_2^R(0)$. It may be observed from the figure that, in the case of

https://doi.org/10.1017/9781108489065.011 Published online by Cambridge University Press

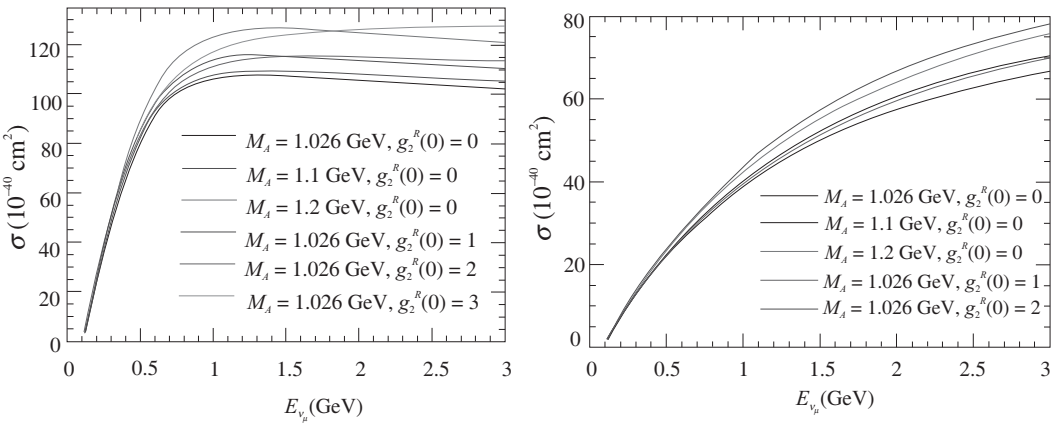

Figure 10.16 σ vs. $E_{\nu_\mu(\bar{\nu}_\mu)}$ for the process $\nu_\mu + n \to \mu^- + p$ (left panel) and $\bar{\nu}_\mu + p \to \mu^+ + n$ (right panel) for different combinations of M_A, and $g_2^R(0)$ viz. $M_A = 1.026$ GeV and $g_2^R(0) = 0$ (solid line), $M_A = 1.1$ GeV and $g_2^R(0) = 0$ (dashed line), $M_A = 1.2$ GeV and $g_2^R(0) = 0$ (dashed dotted line), $M_A = 1.026$ GeV and $g_2^R(0) = 1$ (double dotted dashed line), $M_A = 1.026$ GeV and $g_2^R(0) = 2$ (double dashed dotted line) and $M_A = 1.026$ GeV and $g_2^R(0) = 3$ (dotted line).

neutrino induced processes, that is, $\nu_\mu + n \to \mu^- + p$, the results obtained by taking $M_A = 1.1$ GeV and $g_2^R(0) = 0$ are comparable to the results obtained with $M_A = 1.026$ GeV and $g_2^R(0) = 2$; whereas, the results obtained by taking $M_A = 1.2$ GeV and $g_2^R(0) = 0$ are comparable to the results obtained using $M_A = 1.026$ GeV and $g_2^R(0) = 3$. In the case of an antineutrino induced process, that is, $\bar{\nu}_\mu + p \to \mu^+ + n$, the results obtained by taking $M_A = 1.1$ GeV and $g_2^R(0) = 0$ are comparable to the results obtained with $M_A = 1.026$ GeV and $g_2^R(0) = 1$; whereas, the results obtained by taking $M_A = 1.2$ GeV and $g_2^R(0) = 0$ are slightly lower than the results obtained using $M_A = 1.026$ GeV and $g_2^R(0) = 2$. Thus, a higher value of $\sigma(E_{\bar{\nu}_\mu})$ may be obtained by either taking a non-zero value of $g_2^R(0)$ or increasing the value of M_A. Therefore, the value of M_A depends upon the assumptions made about the value of $g_2^R(0)$. Furthermore, the cross section measurements may give information only about the non-zero value of $g_2^R(0)$ irrespective of the nature of the SCC current, that is, with or without time reversal invariance. One may obtain the nature of the SCC by measuring the polarization observables which give different results with the real and imaginary values of $g_2^R(0)$, corresponding to the SCC with or without time reversal invariance.

10.6 Quasielastic Hyperon Production

10.6.1 Matrix elements and form factors

Quasielastic hyperon production processes are forbidden in the neutrino induced processes due to the $\Delta S \neq \Delta Q$ rule, but are possible with antineutrinos as discussed in Chapter 6. The following processes are induced when an antineutrino interacts with a nucleon to produce a hyperon and an antilepton (Figure 10.17):

$$\bar{\nu}_l(k) + p(p) \quad \to \quad l^+(k') + \Lambda(p'), \tag{10.97}$$

https://doi.org/10.1017/9781108489065.011 Published online by Cambridge University Press

$$\bar{\nu}_l(k) + p(p) \rightarrow l^+(k') + \Sigma^0(p'), \tag{10.98}$$

$$\bar{\nu}_l(k) + n(p) \rightarrow l^+(k') + \Sigma^-(p'), \qquad l = e, \mu, \tau, \tag{10.99}$$

where the quantities in the brackets represent the four momenta of the particles. The transition matrix element for the processes presented in Eqs. (10.97)–(10.99) is written as

$$\mathcal{M} = \frac{G_F}{\sqrt{2}} \sin\theta_c \, l^\mu J_\mu. \tag{10.100}$$

The leptonic current (l^μ) is given in Eq. (10.67). The hadronic current (J_μ) for the quasielastic hyperon production can be written in analogy with the antineutrino–nucleon scattering except that the mass of the final nucleon is replaced by the mass of the hyperon and the electroweak form factors of the nucleons are replaced by the $N - Y$ transition form factors. In general, J_μ is given in Eq. (10.68) with Γ_μ defined in Eq. (10.69). The matrix elements of the vector (V_μ) and the axial vector (A_μ) currents between a hyperon $Y(= \Lambda, \Sigma^0,$ and $\Sigma^-)$ and a nucleon $N = n, p$ are written as:

$$\begin{aligned} \langle Y(\vec{p}\,')|V_\mu|N(\vec{p})\rangle &= \bar{u}(\vec{p}\,') \left[\gamma_\mu f_1^{NY}(q^2) + i\sigma_{\mu\nu}\frac{q^\nu}{M+M'} f_2^{NY}(q^2)\right. \\ &+ \left.\frac{2\,q_\mu}{M+M'} f_3^{NY}(q^2)\right] u(\vec{p}), \end{aligned} \tag{10.101}$$

$$\begin{aligned} \langle Y(\vec{p}\,')|A_\mu|N(\vec{p})\rangle &= \bar{u}(\vec{p}\,') \left[\gamma_\mu\gamma_5 g_1^{NY}(q^2) + i\sigma_{\mu\nu}\frac{q^\nu}{M+M'}\gamma_5 g_2^{NY}(q^2)\right. \\ &+ \left.\frac{2\,q_\mu}{M+M'}\gamma_5 g_3^{NY}(q^2)\right] u(\vec{p}), \end{aligned} \tag{10.102}$$

where M and M' are the masses of the nucleon and hyperon, respectively. $f_1^{NY}(q^2)$, $f_2^{NY}(q^2)$ and $f_3^{NY}(q^2)$ are the vector, weak magnetic, and induced scalar $N - Y$ transition form factors. $g_1^{NY}(q^2)$, $g_2^{NY}(q^2)$ and $g_3^{NY}(q^2)$ are the axial vector, induced tensor (or weak electric), and induced pseudoscalar form factors, respectively.

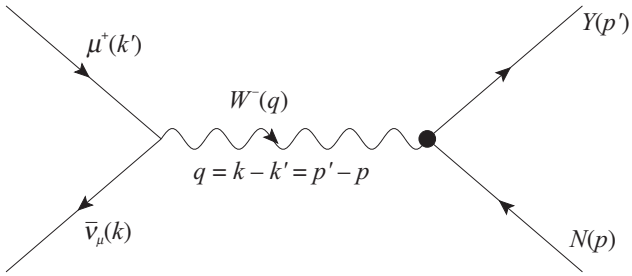

Figure 10.17 Feynman diagram for the process $\bar{\nu}_l(k) + N(p) \rightarrow l^+(k') + Y(p')$, where $N(= p, n)$ and $Y(= \Lambda, \Sigma^0, \Sigma^-)$ represents the initial nucleon and the final hyperon, respectively.

The transition matrix element squared is obtained as

$$\overline{\sum}\sum|\mathcal{M}|^2 = \frac{G_F^2 \sin^2\theta_c}{2} J^{\mu\nu} L_{\mu\nu}, \tag{10.103}$$

https://doi.org/10.1017/9781108489065.011 Published online by Cambridge University Press

where $J^{\mu\nu}$ and $L_{\mu\nu}$ are obtained in a similar way, as mentioned in Section 10.5.3.

The differential scattering cross section $d\sigma/dq^2$ for the processes given in Eq. (10.97)–(10.99) in the Lab frame is then obtained as

$$\frac{d\sigma}{dq^2} = \frac{G_F^2 \sin^2\theta_c}{8\pi M^2 E_{\bar{\nu}_l}^2} N(q^2), \tag{10.104}$$

where $N(q^2) = J^{\mu\nu}L_{\mu\nu}$. It is given in Appendix F.

The weak transition form factors $f_i(q^2)$ and $g_i(q^2)$, $i = 1-3$, are determined using the Cabibbo theory of $V-A$ interaction extended to the strange sector. The details are given in Chapter 6 and Appendix B.

10.6.2 Vector form factors

The expressions for the vector form factors in terms of the electromagnetic form factors $F_{1,2}^p(q^2)$ and $F_{1,2}^n(q^2)$ for the various processes given in Eqs. (10.97)–(10.99), are obtained using SU(3) symmetry in the Cabibbo model. The details are given in Appendix B. These form factors are as follows:

$$f_{1,2}^{p\Lambda}(q^2) = -\sqrt{\frac{3}{2}}\, F_{1,2}^p(q^2), \tag{10.105}$$

$$f_{1,2}^{n\Sigma^-}(q^2) = -\left[F_{1,2}^p(q^2) + 2F_{1,2}^n(q^2)\right], \tag{10.106}$$

$$f_{1,2}^{p\Sigma^0}(q^2) = -\frac{1}{\sqrt{2}}\left[F_{1,2}^p(q^2) + 2F_{1,2}^n(q^2)\right]. \tag{10.107}$$

10.6.3 Axial vector form factors

The axial vector form factors $g_i^{NY}(q^2)(i = 1,2,3)$ are expressed in terms of the two functions $F_i^A(q^2)$ and $D_i^A(q^2)$ corresponding to the antisymmetric and symmetric couplings of the two octets. However, we express the form factors $g_i^{NY}(q^2)$ in terms of $g_i(q^2)$ and $x_i(q^2)$ which are defined as

$$g_i(q^2) = F_i^A(q^2) + D_i^A(q^2), \tag{10.108}$$

$$x_i(q^2) = \frac{F_i^A(q^2)}{F_i^A(q^2) + D_i^A(q^2)}, \qquad i = 1-3. \tag{10.109}$$

The expressions for the axial vector transition form factors for the various processes given in Eqs. (10.97)–(10.99) are given as:

$$g_{1,2}^{p\Lambda}(q^2) = -\frac{1}{\sqrt{6}}(1+2x_{1,2})g_{1,2}(q^2), \tag{10.110}$$

$$g_{1,2}^{n\Sigma^-}(q^2) = (1-2x_{1,2})g_{1,2}(q^2), \tag{10.111}$$

$$g_{1,2}^{p\Sigma^0}(q^2) = \frac{1}{\sqrt{2}}(1-2x_{1,2})g_{1,2}(q^2). \tag{10.112}$$

https://doi.org/10.1017/9781108489065.011 Published online by Cambridge University Press

In the following, we describe the explicit forms of the axial vector form factors used for calculating the numerical results.

(a) Axial vector form factor $g_1^{NY}(q^2)$
We note from Eq. (10.108) that $g_1(q^2)$ is the axial vector form factor for $n \to p$ transition. It is defined in Eq. (10.86). The parameter $x_1(q^2)$ occurring in Eqs. (10.110)–(10.112) for $g_1^{NY}(q^2)$ ($Y = \Lambda, \Sigma^0, \Sigma^-$) is determined at low Q^2 from the analysis of semileptonic hyperon decay (SHD) and is found to be $x_1(Q^2 \approx 0) = 0.364$. There is no experimental information about the Q^2 dependence of $x_1(q^2)$; therefore, we assume it to be constant, that is, $x_1(q^2) \approx x_1(0) = 0.364$ for convenience.

(b) Second class current form factor $g_2^{NY}(q^2)$
The expression for $g_2^{NY}(q^2)$ for the hyperons $\Lambda, \Sigma^-, \Sigma^0$ are given in Eqs. (10.110)–(10.112) in terms of $g_2(q^2)$ and $x_2(q^2)$, where $g_2(q^2)$ is parameterized in Eq. (10.91). There is some information about $g_2(q^2)$ from the neutrino and antineutrino scattering off the nucleons. It is known that the determination of the experimental value of $g_2(0)$ is correlated with the value of $M_2 (= M_A)$ (Eq. (10.91)) used in the analysis. There exist theoretical calculations for $g_2^{R(np)}(0)$ and $g_2^{R(NY)}(0)$ for $Y = \Lambda, \Sigma^-, \Sigma^0$. In the literature, various values of $g_2^I(0)$ for nucleons and hyperons have been used, which are in the range 1–10 [448, 449, 450]. However, there is no information about $x_2(q^2)$. To see the dependence of $g_2^R(0)$ and $g_2^I(0)$ on the differential and the total scattering cross section, we have varied $g_2^R(0)$ and $g_2^I(0)$ in the range $0 - 3$ and used $M_2 = M_A$. For the q^2 dependence of the form factor, that is, $g_2^{NY}(q^2)$, we use the SU(3) symmetric expressions for $g_2(q^2)$ taken to be of dipole form given in Eq. (10.91) for the various transitions given in Eqs. (10.110)–(10.112), treating $x_2(q^2)$ to be constant. Let us take $x_2 = x_1$ for simplicity.

(c) The induced pseudoscalar form factor $g_3^{NY}(q^2)$
In general, the contribution of $g_3(q^2)$ to the (anti)neutrino scattering cross sections is proportional to m_l^2, where m_l is the mass of the corresponding charged lepton, and is small in e^- and μ^- induced processes. It is significant in the process involving τ^- leptons. For $g_3^{NY}(q^2)$, Nambu [46] has given a generalized parameterization using PCAC and generalized GT relation for the $\Delta S = 1$ currents, that is,

$$g_3^{NY}(q^2) = \frac{(M + M_Y)^2}{2(m_K^2 - q^2)} g_1^{NY}(q^2), \tag{10.113}$$

where m_K is the mass of kaon and $g_1^{NY}(q^2)$ is given in Eqs. (10.110)–(10.112) for $Y = \Lambda, \Sigma^-, \Sigma^0$.

10.6.4 Cross sections: Experimental results

Figure 10.18 presents the results for $\bar{\nu}_\mu$ induced Λ production from the free proton in the energy region of $E_{\bar{\nu}_\mu} < 10$ GeV and compares them with the experimental results from the Gargamelle

https://doi.org/10.1017/9781108489065.011 Published online by Cambridge University Press

bubble chamber at CERN [451, 452, 453] using propane with a small admixture of freon and from Serpukhov SKAT bubble chambers [454] using freon and from the BNL experiment using a hydrogen target [455]. We have presented the theoretical results by taking the different values of $g_2(0)$, viz., $g_2^{R,I}(0) = 0$, $g_2^R(0) = 3$ and $g_2^I(0) = 3$. It may be observed that the non-zero value of $g_2(0)$ (whether real or imaginary) increases the cross section; in the case $g_2^R(0) = 3$ or $g_2^I(0) = 3$, the cross section increases by about 20%.

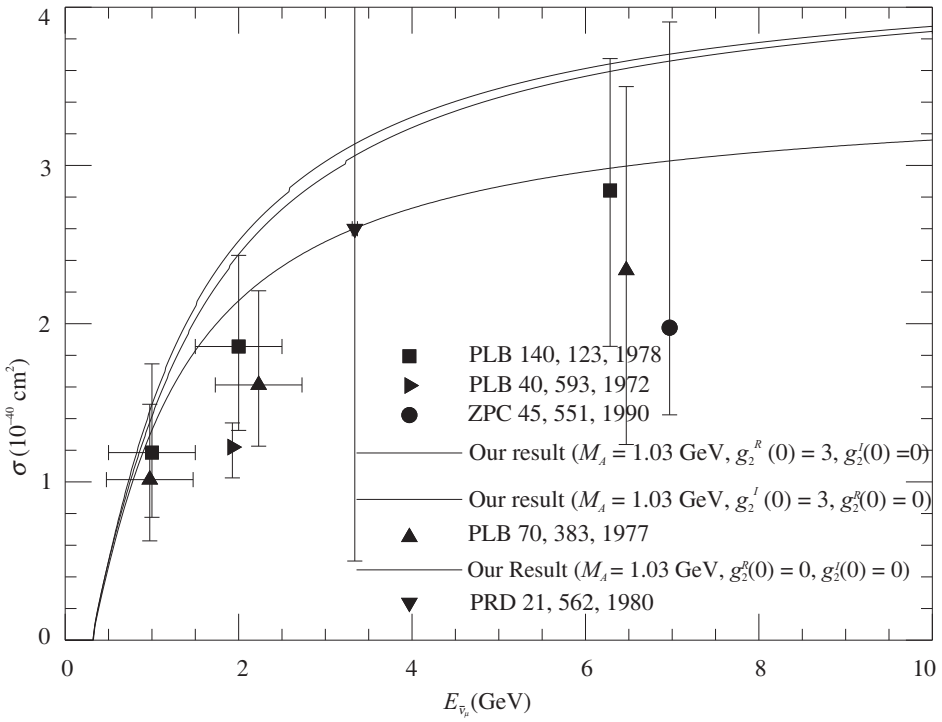

Figure 10.18 σ vs. $E_{\bar{\nu}_\mu}$, for $\bar{\nu}_\mu + p \to \mu^+ + \Lambda$ process. Experimental results (triangle right [451], square [452], triangle up [453], circle [454]), triangle down($\sigma = 2.6^{+5.9}_{-2.1} \times 10^{-40}\text{cm}^2$) [455]) are shown with error bars. The solid line represents the results obtained with $M_A = 1.03$ GeV and $g_2 = 0$ while the dashed (double dotted dashed line) represents the results obtained with $M_A = 1.03$ GeV and $g_2^R(0) = 3$ ($g_2^I(0) = 3$).

10.7 Polarization of Final Hadrons and Leptons

10.7.1 Introduction

In elastic $e^- p$ scattering, the experiments with polarized electron beam and the polarized proton target play an important role in determining the vector form factors. In the weak sector, the vector form factors are expressed in terms of the electromagnetic form factors of the nucleons. In the axial vector sector, information about the form factors is obtained from the semileptonic decays of nucleons and hyperons at low q^2. One may also obtain information about these form factors by measuring the polarization of the final hadron. Experimentally, it is difficult to study

https://doi.org/10.1017/9781108489065.011 Published online by Cambridge University Press

polarization of the final nucleon in quasielastic ($\Delta S = 0$) scattering as one requires a double scattering measurement. However, it is easier to study polarization observables in quasielastic hyperon production as the produced hyperons decay into pions which gives information about the polarization of the hyperon.

10.7.2 Polarization of the final hadron

The polarization four-vector ξ^τ of the hadron produced in the final state in the reactions shown in Eqs. (10.97)–(10.99) is written as (Appendix C and Ref. [456] for details):

$$\xi^\tau = \frac{\mathrm{Tr}[\gamma^\tau\gamma_5\,\rho_f(p')]}{\mathrm{Tr}[\rho_f(p')]}, \tag{10.114}$$

where the spin density matrix $\rho_f(p')$ corresponding to the final hadron of momentum p' is given by

$$\rho_f(p') = L^{\alpha\beta}\,\mathrm{Tr}[\Lambda(p')\Gamma_\alpha\Lambda(p)\tilde{\Gamma}_\beta\Lambda(p')]. \tag{10.115}$$

In this expression, Γ_α is given in Eq. (10.69). Using the following relations,

$$\Lambda(p')\gamma^\tau\gamma_5\Lambda(p') = 2M'\left(g^{\tau\sigma} - \frac{p'^\tau p'^\sigma}{M'^2}\right)\Lambda(p')\gamma_\sigma\gamma_5, \tag{10.116}$$

$$\Lambda(p')\Lambda(p') = 2M'\Lambda(p'), \tag{10.117}$$

where M' corresponds to the mass of the final hadron, ξ^τ defined in Eq. (10.114) may be rewritten as (Appendix C):

$$\xi^\tau = \left(g^{\tau\sigma} - \frac{p'^\tau p'^\sigma}{M'^2}\right)\frac{L^{\alpha\beta}\mathrm{Tr}\left[\gamma_\sigma\gamma_5\Lambda(p')\Gamma_\alpha\Lambda(p)\tilde{\Gamma}_\beta\right]}{L^{\alpha\beta}\mathrm{Tr}\left[\Lambda(p')\Gamma_\alpha\Lambda(p)\tilde{\Gamma}_\beta\right]}. \tag{10.118}$$

Note that in Eq. (10.118), ξ^τ is manifestly orthogonal to p'^τ, that is, $p'\cdot\xi = 0$. Moreover, the denominator is directly related to the differential scattering cross section given in Eq. (10.104).

With $J^{\alpha\beta}$ and $L_{\alpha\beta}$ given in Eqs. (10.74) and (10.73), respectively, an expression for ξ^τ is obtained in terms of the four-momenta of the particles. Here, we have considered two cases:

Case I: When time reversal invariance is assumed.
We evaluate the polarization vector ξ^τ defined in Eq. (10.118) in the lab frame, that is, when the initial nucleon is at rest, $\vec{p} = 0$. Moreover, from the momentum conservation, $\vec{k}'$ is resolved in terms of $\vec{k}$, $\vec{p}$, and $\vec{p}\,'$. If the time reversal invariance is assumed, then all the form factors defined in Eq. (10.69) are real and the polarization vector can be expressed as

$$\vec{\xi} = \frac{\left[A^h(q^2)\vec{k} + B^h(q^2)\vec{p}\,'\right]}{N(q^2)}, \tag{10.119}$$

https://doi.org/10.1017/9781108489065.011 Published online by Cambridge University Press

where the expressions of $A^h(q^2)$, $B^h(q^2)$, and $N(q^2)$ are given in Appendix F. In Eq. (10.119), $A^h(q^2)$, $B^h(q^2)$, and $N(q^2)$ given in Appendix F are taken in the limit $f_3(q^2) = 0$ and $g_2(0) = g_2^R(0)$ to ensure the time reversal invariance.

From Eq. (10.119), it follows that the polarization lies in the plane of reaction and there is no component of polarization in a direction perpendicular to the reaction plane. This is a consequence of time reversal invariance which makes the transverse polarization in the direction perpendicular to the reaction plane vanish. We now expand the polarization vector $\vec{\xi}$ along the orthogonal directions, $\hat{e}_L^h$, $\hat{e}_P^h$, and $\hat{e}_T^h$ in the reaction plane corresponding to the longitudinal, perpendicular, and transverse directions, defined as

$$\hat{e}_L^h = \frac{\vec{p}\,'}{|\vec{p}\,'|}, \qquad \hat{e}_P^h = \hat{e}_L^h \times \hat{e}_T^h, \qquad \text{where} \quad \hat{e}_T^h = \frac{\vec{p}\,' \times \vec{k}}{|\vec{p}\,' \times \vec{k}|}, \tag{10.120}$$

and depicted in Figure 10.19(b). We then write $\vec{\xi}$ as:

$$\vec{\xi} = \xi_L \hat{e}_L^h + \xi_P \hat{e}_P^h, \tag{10.121}$$

such that the longitudinal and perpendicular components of the polarization vector ($\vec{\xi}$) in the laboratory frame are given by

$$\xi_L(q^2) = \vec{\xi} \cdot \hat{e}_L^h, \qquad \xi_P(q^2) = \vec{\xi} \cdot \hat{e}_P^h. \tag{10.122}$$

From Eq. (10.122), the longitudinal $P_L^h(q^2)$ and perpendicular $P_P^h(q^2)$ components of the polarization vector defined in the rest frame of the final hadron are given by

$$P_L^h(q^2) = \frac{M'}{E_{p'}} \xi_L(q^2), \qquad P_P^h(q^2) = \xi_P(q^2), \tag{10.123}$$

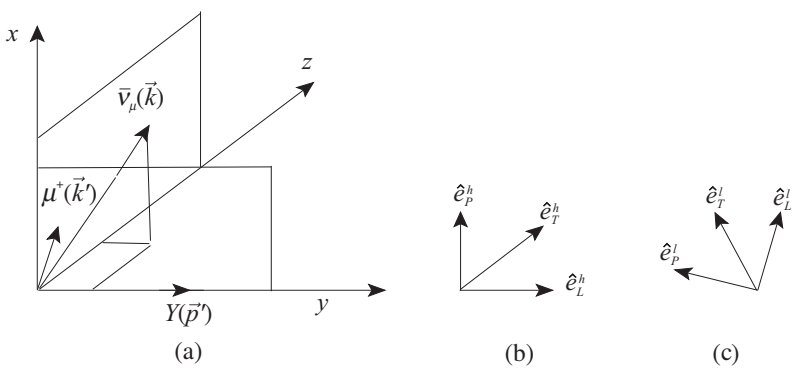

Figure 10.19 (a) Momentum and polarization directions of the final baryon and lepton. $\hat{e}_L^{h,l}$, $\hat{e}_P^{h,l}$, and $\hat{e}_T^{h,l}$ represent the orthogonal unit vectors corresponding to the longitudinal, perpendicular, and transverse directions with respect to the momentum of the final hadron in (b) and the final lepton in (c).

https://doi.org/10.1017/9781108489065.011 Published online by Cambridge University Press

where $\frac{M'}{E_{p'}}$ is the Lorentz boost factor along $\vec{p}\,'$. With the help of Eqs. (10.119), (10.120), (10.122), and (10.123), the longitudinal $P_L^h(q^2)$ and perpendicular $P_P^h(q^2)$ components are calculated to be:

$$P_L^h(q^2) = \frac{M'}{E_{p'}} \frac{A^h(q^2)\vec{k}\cdot\vec{p}\,' + B^h(q^2)|\vec{p}\,'|^2}{N(q^2)\,|\vec{p}\,'|}, \tag{10.124}$$

$$P_P^h(q^2) = \frac{A^h(q^2)[(\vec{k}\cdot\vec{p}\,')^2 - |\vec{k}|^2|\vec{p}\,'|^2]}{N(q^2)\,|\vec{p}\,'|\,|\vec{p}\,'\times\vec{k}|}. \tag{10.125}$$

To see the dependence of $g_2^R(0)$ on the polarization observables, the results for $P_L^\Lambda(Q^2)$ and $P_P^\Lambda(Q^2)$ are presented as a function of Q^2 in Figure 10.20 for the process $\bar{\nu}_\mu + p \to \mu^+ + \Lambda$ using $g_2^R(0) = 0, \pm 1$, and ± 3 at $E_{\bar{\nu}_\mu} = 1$ GeV. It may be observed that $P_L^\Lambda(Q^2)$ shows large variations as we change $|g_2^R(0)|$ from 0 to 3. For example, in the peak region of Q^2, the difference is about 50% as $|g_2^R(0)|$ is changed from 0 to 3. In the case of $P_P^\Lambda(Q^2)$ also, the Q^2 dependence is quite strong and similar to $P_L^\Lambda(Q^2)$.

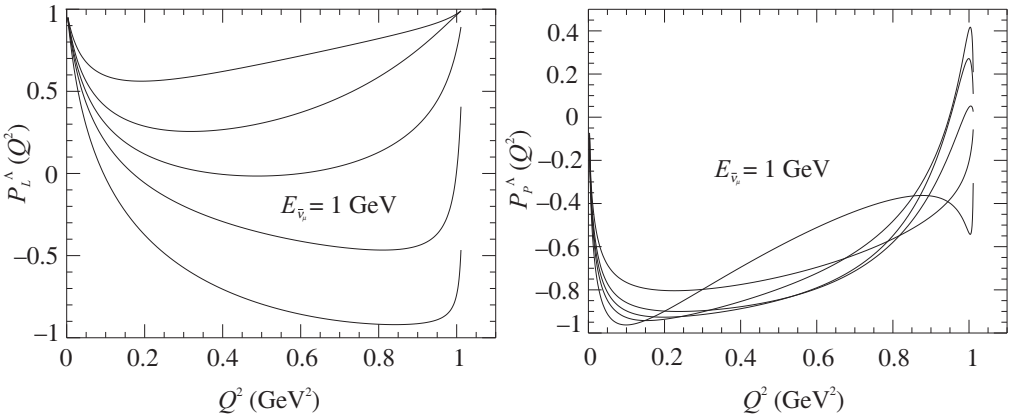

Figure 10.20 $P_L^\Lambda(Q^2)$ vs. Q^2 (left panel) and $P_P^\Lambda(Q^2)$ vs. Q^2 (right panel) for the process $\bar{\nu}_\mu + p \to \mu^+ + \Lambda$ at the incoming antineutrino energy, $E_{\bar{\nu}_\mu} = 1$ GeV for the polarized Λ in the final state, at different values of $g_2^R(0)$, viz., $g_2^R(0) = 0$ (solid line), 1 (dashed line), 3 (dashed dotted line), -1 (double dotted dashed line) and -3 (double dashed dotted line).

Case II: When time reversal violation is assumed.
In the absence of time reversal invariance, the polarization vector $\vec{\xi}$ is calculated as

$$\begin{aligned}\vec{\xi} &= \frac{A^h(q^2)\vec{k} + B^h(q^2)\vec{p}\,' + C^h(q^2)\epsilon^{\alpha\beta\gamma\delta}k_\beta p_\gamma p'_\delta}{N(q^2)} \\ &= \frac{A^h(q^2)\vec{k} + B^h(q^2)\vec{p}\,' + C^h(q^2)[\epsilon^{ijk}k_j p'_k M]}{N(q^2)} \\ &= \frac{A^h(q^2)\vec{k} + B^h(q^2)\vec{p}\,' + C^h(q^2)M(\vec{k}\times\vec{p}\,')}{N(q^2)},\end{aligned} \tag{10.126}$$

https://doi.org/10.1017/9781108489065.011 Published online by Cambridge University Press

where the expressions of $C^h(q^2)$ is given in Appendix F.

The polarization vector $\vec{\xi}$ may be written in terms of the longitudinal, perpendicular, and transverse components as

$$\vec{\xi} = \xi_L \hat{e}_L^h + \xi_P \hat{e}_P^h + \xi_T \hat{e}_T^h, \tag{10.127}$$

where the unit vectors are defined in Eq. (10.120). The longitudinal and perpendicular components are given in Eqs. (10.124) and (10.125), respectively. The transverse component of polarization in the rest frame of the final hadron is given as

$$P_T(q^2) = \xi_T(q^2) = \vec{\xi}.\hat{e}_T. \tag{10.128}$$

Using Eqs. (10.120) and (10.127) in Eq. (10.128), we obtain

$$P_T^h(q^2) = \frac{C^h(q^2) M[(\vec{k}\cdot\vec{p}\,')^2 - |\vec{k}|^2|\vec{p}\,'|^2]}{N(q^2)\,|\vec{p}\,'\times\vec{k}|}. \tag{10.129}$$

If the time reversal invariance (TRI) is assumed, then all the vector and the axial vector form factors are real and the expression for $C^h(q^2)$ (given in Appendix F) vanishes which implies that the transverse component of the polarization perpendicular to the production plane, $P_T^h(q^2)$ vanishes.

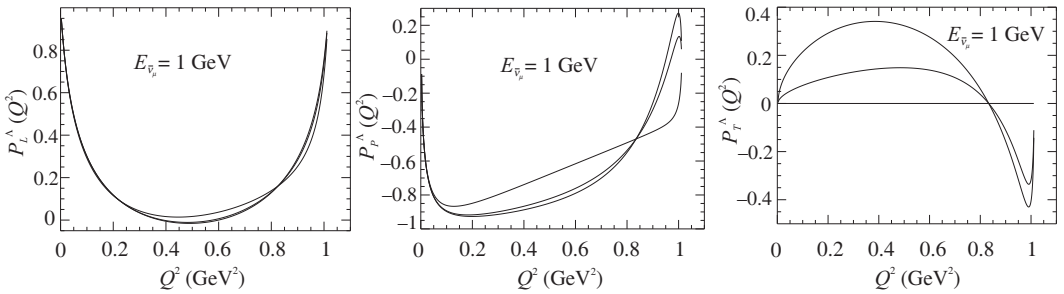

Figure 10.21 $P_L^\Lambda(Q^2)$ vs. Q^2 (left panel), $P_P^\Lambda(Q^2)$ vs. Q^2 (middle panel) and $P_T^\Lambda(Q^2)$ vs. Q^2 (right panel) for the process $\bar{\nu}_\mu + p \to \mu^+ + \Lambda$ at the incoming antineutrino energy, $E_{\bar{\nu}_\mu} = 1$ GeV for the polarized Λ in the final state, at different values of $g_2^I(0)$, viz., $g_2^I(0) = 0$ (solid line), 1 (dashed line), and 3 (dashed dotted line).

To see the dependence of $g_2^I(0)$ on the polarization observables, the results are presented in Figure 10.21 for $P_L^\Lambda(Q^2)$, $P_P^\Lambda(Q^2)$, and $P_T^\Lambda(Q^2)$ as a function of Q^2 using $g_2^I(0) = 0$, 1, and 3 at $E_{\bar{\nu}_\mu} = 1$ GeV. It may be deduced that while $P_L^\Lambda(Q^2)$ is less sensitive to $g_2^I(0)$ at low antineutrino energies, $P_P^\Lambda(Q^2)$ is sensitive to $g_2^I(0)$ at $E_{\bar{\nu}_\mu} = 1$ GeV. Moreover, $P_T^\Lambda(Q^2)$ shows 40% variations at $Q^2 = 0.4$ GeV^2, $E_{\bar{\nu}_\mu} = 1$ GeV, when $g_2^I(0)$ is varied from 0 to 3.

https://doi.org/10.1017/9781108489065.011 Published online by Cambridge University Press

10.7.3 Polarization of the final lepton

Instead of the final hadron polarization, if one assumes the final lepton to be polarized, then the polarization four-vector(ζ^τ) in reactions, Eqs. (10.97)–(10.99) is written as

$$\zeta^\tau = \frac{\mathrm{Tr}[\gamma^\tau\gamma_5\,\rho_f(k')]}{\mathrm{Tr}[\rho_f(k')]}, \tag{10.130}$$

and the spin density matrix for the final lepton $\rho_f(k')$ is given by

$$\rho_f(k') = J^{\alpha\beta}\,\mathrm{Tr}[\Lambda(k')\gamma_\alpha(1+\gamma_5)\Lambda(k)\tilde{\gamma}_\beta(1+\tilde{\gamma}_5)\Lambda(k')], \tag{10.131}$$

with $\tilde{\gamma}_\alpha = \gamma^0\gamma_\alpha^\dagger\gamma^0$ and $\tilde{\gamma}_5 = \gamma^0\gamma_5^\dagger\gamma^0$.

Using Eqs. (10.116) and (10.117), ζ^τ defined in Eq. (10.130) may also be rewritten as

$$\zeta^\tau = \left(g^{\tau\sigma} - \frac{k'^\tau k'^\sigma}{m_l^2}\right)\frac{J^{\alpha\beta}\mathrm{Tr}\left[\gamma_\sigma\gamma_5\Lambda(k')\gamma_\alpha(1+\gamma_5)\Lambda(k)\tilde{\gamma}_\beta(1+\tilde{\gamma}_5)\right]}{J^{\alpha\beta}\mathrm{Tr}\left[\Lambda(k')\gamma_\alpha(1+\gamma_5)\Lambda(k)\tilde{\gamma}_\beta(1+\tilde{\gamma}_5)\right]}, \tag{10.132}$$

where m_l is the charged lepton mass. In Eq. (10.132), the denominator is directly related to the differential scattering cross section given in Eq. (10.104).

With $J^{\alpha\beta}$ and $L_{\alpha\beta}$ given in Eqs. (10.74) and (10.73), respectively, an expression for ζ^τ is obtained. In the laboratory frame, where the initial nucleon is at rest, the polarization vector $\vec{\zeta}$ is calculated to be a function of three-momenta of incoming antineutrino ($\vec{k}$) and outgoing lepton ($\vec{k}\,'$), and is given as

$$\vec{\zeta} = \frac{\left[A^l(q^2)\vec{k} + B^l(q^2)\vec{k}\,' + C^l(q^2)M(\vec{k}\times\vec{k}\,')\right]}{N(q^2)}, \tag{10.133}$$

where the expressions of $A^l(q^2)$, $B^l(q^2)$, and $C^l(q^2)$ are given in Appendix F.

One may expand the polarization vector $\vec{\zeta}$ along the orthogonal directions, $\hat{e}_L^l$, $\hat{e}_P^l$, and $\hat{e}_T^l$ in the reaction plane corresponding to the longitudinal, perpendicular, and transverse directions, defined as

$$\hat{e}_L^l = \frac{\vec{k}'}{|\vec{k}'|}, \qquad \hat{e}_P^l = \hat{e}_L^l \times \hat{e}_T^l, \qquad \text{where} \quad \hat{e}_T^l = \frac{\vec{k}\times\vec{k}'}{|\vec{k}\times\vec{k}'|}, \tag{10.134}$$

and depicted in Figure 10.19(c). We then write $\vec{\zeta}$ as:

$$\vec{\zeta} = \zeta_L\hat{e}_L^l + \zeta_P\hat{e}_P^l + \zeta_T\hat{e}_T^l, \tag{10.135}$$

https://doi.org/10.1017/9781108489065.011 Published online by Cambridge University Press

such that the longitudinal, perpendicular, and transverse components of the $\vec{\zeta}$ in the laboratory frame are given by

$$\zeta_L(q^2) = \vec{\zeta}\cdot\hat{e}^l_L, \qquad \zeta_P(q^2) = \vec{\zeta}\cdot\hat{e}^l_P, \qquad \zeta_T(q^2) = \vec{\zeta}\cdot\hat{e}^l_T. \tag{10.136}$$

From Eq. (10.136), the longitudinal $P^l_L(q^2)$, perpendicular $P^l_P(q^2)$, and transverse $P^l_T(q^2)$ components of the polarization vector defined in the rest frame of the final lepton are given by

$$P^l_L(q^2) = \frac{m_l}{E_{k'}}\zeta_L(q^2), \qquad P^l_P(q^2) = \zeta_P(q^2), \qquad P^l_T(q^2) = \zeta_T(q^2), \tag{10.137}$$

where $\frac{m_l}{E_{k'}}$ is the Lorentz boost factor along $\vec{k}'$. Using Eqs. (10.133), (10.134), and (10.136) in Eq. (10.137), the longitudinal $P^l_L(q^2)$, perpendicular $P^l_P(q^2)$, and transverse $P^l_T(q^2)$ components are calculated to be

$$P^l_L(q^2) = \frac{m_\mu}{E_{k'}}\frac{A^l(q^2)\vec{k}\cdot\vec{k}' + B^l(q^2)|\vec{k}'|^2}{N(q^2)\ |\vec{k}'|}, \tag{10.138}$$

$$P^l_P(q^2) = \frac{A^l(q^2)[|\vec{k}|^2|\vec{k}'|^2 - (\vec{k}\cdot\vec{k}')^2]}{N(q^2)\ |\vec{k}'|\ |\vec{k}\times\vec{k}'|}, \tag{10.139}$$

$$P^l_T(q^2) = \frac{C^l(q^2)M[(\vec{k}\cdot\vec{k}')^2 - |\vec{k}|^2|\vec{k}'|^2]}{N(q^2)\ |\vec{k}\times\vec{k}'|}. \tag{10.140}$$

The lepton polarization observables do not give any significant information about T-noninvariance as they are very small and difficult to measure. In the case of τ-lepton, the polarization of τ will be substantial because of its mass but the experiments are very difficult to perform at the present time.

https://doi.org/10.1017/9781108489065.011 Published online by Cambridge University Press